

Post-shutdown cooling of sodium-cooled trench-type
reactor vessel outer walls by natural circulation of gas

by

Anil P. Macwan

A Thesis Submitted to the
Graduate Faculty in Partial Fulfillment of the
Requirements for the Degree of
MASTER OF SCIENCE

Major: Nuclear Engineering

Signatures have been redacted for privacy

Iowa State University
Ames, Iowa

1987

TABLE OF CONTENTS

	PAGE
NOMENCLATURE	ix
1. INTRODUCTION	1
2. DESCRIPTION OF THE SYSTEM	4
2.1 The Trench Reactor	4
2.2 Decay Heat Produced in a Reactor	6
2.3 Shutdown Cooling of the Trench Reactor	7
2.4 Natural Circulation Loop	8
3. METHOD OF SOLUTION	12
3.1. The Problem	12
3.2. Assumptions	14
3.3 Method of Solution and Governing Equations	19
3.3.1 Iterative procedure and nodal method	23
3.3.2 Transient behavior of wall temperature	34
4. RESULTS AND DISCUSSION	37
4.1 Results of the Iterative Procedure	38
4.1.1 Total heat removal rate as a function of reactor wall temperature	38
4.1.2 Baffle temperature as a function of reactor wall temperature	42
4.1.3 Channel outlet gas temperature as a function of wall temperature	46
4.2 Transient Behavior of the System	55
4.2.1 Reactor wall temperature as a function of time	56
4.2.2 Baffle temperature and gas outlet temperature as a function of time	58
5. CRITICAL EVALUATION, SUMMARY AND CONCLUSIONS	68
5.1 Critical Evaluation of Present Study	68
5.2 Summary and Conclusions	70
6. SUGGESTIONS FOR FUTURE WORK	73
7. BIBLIOGRAPHY	79
8. ACKNOWLEDGEMENT	81
9. APPENDIX A. CALCULATION OF RALEIGH NUMBER FOR THE INNER CHANNEL	82
10. APPENDIX B. COMPARISON OF HEAT GENERATION TERM USED IN PRESENT ANALYSIS WITH TABULATED RESULTS	84

11. APPENDIX C. FORMULA FOR VIEW FACTOR BETWEEN REACTOR WALLS AND BAFFLE	86
12. APPENDIX D. PROGRAM TO PERFORM ITERATIVE PROCEDURE	87
13. APPENDIX E. PROGRAM USING ODEPACK TO SOLVE DIFFERENTIAL EQUATION 3.38	93
14. APPENDIX F. RESULTS OF COMPUTATIONS USING ITERATIVE PROCEDURE	96
15. APPENDIX G. RESULTS OF COMPUTATIONS USING ODEPACK .	102

LIST OF TABLES

	PAGE
TABLE 1. Values of Gr and Ra for the Inner Channel . . .	83
TABLE 2. Comparison of Decay Heat Calculated from semi-empirical correlation and Obtained from Table in ref. [5]	85
TABLE 3. Effect of D and T_w on Heat Removal Rate	96
TABLE 4. Effect of ϵ and T_w on Heat Removal Rate	96
TABLE 5. Effect of Ω and T_w on Heat Removal Rate	97
TABLE 6. Effect of $T_{g,i}$ and T_w on Heat Removal Rate	97
TABLE 7. Effect of D and T_w on Baffle Temperature	98
TABLE 8. Effect of ϵ and T_w on Baffle Temperature	98
TABLE 9. Effect of Ω and T_w on Baffle Temperature	99
TABLE 10. Effect of $T_{g,i}$ and T_w on Baffle Temperature	99
TABLE 11. Effect of D and T_w on Outlet Gas Temperature	100
TABLE 12. Effect of ϵ and T_w on Outlet Gas Temperature	100
TABLE 13. Effect of Ω and T_w on Outlet Gas Temperature	101
TABLE 14. Effect of $T_{g,i}$ and T_w on Outlet Gas Temperature	101
TABLE 15. T_w as a function of θ with no cooling	102
TABLE 16. T_w as a function of θ and D	102
TABLE 17. T_w as a function of θ and ϵ	103
TABLE 18. T_w as a function of θ and Ω	104

TABLE 19. T_b as a function of θ and D	104
TABLE 20. T_b as a function of θ and ϵ	105
TABLE 21. T_b as a function of θ and Ω	106
TABLE 22. T_{g_o} as a function of θ and D	106
TABLE 23. T_{g_o} as a function of θ and ϵ	107
TABLE 24. T_{g_o} as a function of θ and Ω	108

LIST OF FIGURES

	PAGE
FIGURE 1. Cross Section Views of the Trench Reactor [7]	5
FIGURE 2. Schematic views of the Natural Circulation Loop	10
FIGURE 3. Modes of Heat Transfer for the Inner Channel	13
FIGURE 4. Nodal Representation of the Inner Channel . .	24
FIGURE 5. Total Heat Removal Rate versus Wall Temperature for different values D, with ϵ = 0.7, Ω = 0.5 and $T_{g,i}$ = 37.78° C	40
FIGURE 6. Total Heat Removal Rate versus Wall Temperature for different values of ϵ , with D = 1.5 ft, Ω = 0.5 and $T_{g,i}$ = 37.78° C	41
FIGURE 7. Total Heat Removal Rate versus Wall Temperature for different values of Ω , with D = 1.5 ft, ϵ = 0.7 and $T_{g,i}$ = 37.78° C	43
FIGURE 8. Total Heat Removal Rate versus Wall Temperature for different values of $T_{g,i}$, with D = 1.5 ft, ϵ = 0.7 and Ω = 0.5	44
FIGURE 9. Baffle Temperature versus Wall Temperature for different values of D, with ϵ = 0.7, Ω = 0.5 and $T_{g,i}$ = 37.78° C	45
FIGURE 10. Baffle Temperature versus Wall Temperature for different values of ϵ , with D = 1.5 ft, Ω = 0.5 and $T_{g,i}$ = 37.78° C	47
FIGURE 11. Baffle Temperature versus Wall Temperature for different values of Ω , with D = 1.5 ft, ϵ = 0.7 and $T_{g,i}$ = 37.78° C	48

FIGURE 12.	Baffle Temperature versus Wall Temperature for different values of $T_{g,i}$, with $D = 1.5$ ft, $\epsilon = 0.7$ and $\Omega = 0.5$	49
FIGURE 13.	Channel Outlet Gas Temperature versus Wall Temperature for different values of D , with $\epsilon = 0.7$, $\Omega = 0.5$ and $T_{g,i} = 37.78^\circ$ C	51
FIGURE 14.	Channel Outlet Gas Temperature versus Wall Temperature for different values of ϵ , with $D = 1.5$ ft, $\Omega = 0.5$ and $T_{g,i} = 37.78^\circ$ C	52
FIGURE 15.	Channel Outlet Gas Temperature versus Wall Temperature for different values of Ω , with $D = 1.5$ ft, $\epsilon = 0.7$ and $T_{g,i} = 37.78^\circ$ C	53
FIGURE 16.	Channel Outlet Gas Temperature versus Wall Temperature for different values of $T_{g,i}$, with $D = 1.5$ ft, $\epsilon = 0.7$ and $\Omega = 0.5$	54
FIGURE 17.	Wall Temperature versus Time for different values of D , with $\epsilon = 0.7$, $\Omega = 0.5$ and $T_{g,i} = 37.78^\circ$ C	57
FIGURE 18.	Wall Temperature versus Time for different values of ϵ , with $D = 1.5$ ft, $\Omega = 0.5$ and $T_{g,i} = 37.78^\circ$ C	59
FIGURE 19.	Wall Temperature versus Time for different values of Ω , with $D = 1.5$ ft, $\epsilon = 0.7$ and $T_{g,i} = 37.78^\circ$ C	60
FIGURE 20.	Baffle Temperature versus Time for different values of D , with $\epsilon = 0.7$, $\Omega = 0.5$ and $T_{g,i} = 37.78^\circ$ C	62
FIGURE 21.	Baffle Temperature versus Time for different values of ϵ , with $D = 1.5$ ft, $\Omega = 0.5$ and $T_{g,i} = 37.78^\circ$ C	63
FIGURE 22.	Baffle Temperature versus Time for different values of Ω , with $D = 1.5$ ft, $\epsilon = 0.7$ and $T_{g,i} = 37.78^\circ$ C	64
FIGURE 23.	Gas Outlet Temperature versus Time for different values of D , with $\epsilon = 0.7$, $\Omega = 0.5$ and $T_{g,i} = 37.78^\circ$ C	65

- FIGURE 24. Gas Outlet Temperature versus Time for
different values of ϵ , with $D = 1.5$ ft, Ω
 $= 0.5$ and $T_{g,i} = 37.78^\circ$ C 66
- FIGURE 25. Gas Outlet Temperature versus Time for
different values of Ω , with $D = 1.5$ ft, ϵ
 $= 0.7$ and $T_{g,i} = 37.78^\circ$ C 67
- FIGURE 26. Possible Configurations for the Inner
Channel 78

NOMENCLATURE

- A - area, m^2
- C_p - specific heat, $kcal/kg-^{\circ}C$ (or $^{\circ}K$)
- D - distance between reactor walls and baffle, or diameter, m
- H - height of sodium level in the pool, m
- h - heat transfer coefficient, $W/m^2-^{\circ}C$ (or $^{\circ}K$)
- K - thermal conductivity, $W/m-^{\circ}C$ (or $^{\circ}K$)
- L - length of reactor vessel, m
- M - mass, kg
- m - mass flow rate, kg/s
- P - power, MW
- Q - heat transferred for inner channel, MW
- q - heat transferred for node, MW
- T - temperature, $^{\circ}C$ or $^{\circ}K$
- U - overall heat transfer coefficient, $W/m^2-^{\circ}C$ (or $^{\circ}K$)
- v - velocity, m/s
- W - width of reactor vessel, m
- ΔH - node height, m
- Δp - pressure loss, $kg/m-s^2$
- θ - time after shutdown, s
- μ - viscosity, $kg/m-s$
- ρ - density, kg/m^3
- σ - Stefan-Boltzmann's constant, $W/m^2-^{\circ}K^4$

Dimensionless

F - view factor

f - friction factor

Re - Reynolds number

X - relaxation parameter

Y - relaxation parameter

ϵ - emissivity, or error parameter

Ω - ratio of the pressure drop at entrance-exit to
total pressure drop in the circuit

Subscripts

av - average

b - baffle

bc - convection from baffle to gas

be - value for iteration for baffle

bg - guessed value for baffle

bi - iterated value for baffle

bnew - new value for baffle

bo - overall value for baffle

bold - old value for baffle

e - equivalent

ee - entrance-exit

f - flow,

fric - frictional

g - gas

gav - average for gas

gf - outlet for final node
gi - inlet for gas
gnode - value for gas for node
go - outlet for gas
gw - value for gas at wall temperature
gl - value for gas at node inlet
g2 - value for gas at node outlet
Na - sodium
nb - value for node for baffle
node - value for node
nw - value for node for reactor walls
o - nominal
tot - total
w - reactor walls
wb - between reactor walls and baffle
wc - convection from reactor walls to gas
wr - radiation from reactor walls to baffle

1. INTRODUCTION

The concept of post-shutdown cooling of reactor vessel outer walls by natural circulation of gas has been receiving some attention recently. It is aimed at being applied to shutdown heat removal in advanced liquid metal reactor concepts. Atomic International (AI) and General Electric (GE) have been selected by Department of Energy to develop their innovative design concepts aimed at improving safety, lowering plant costs, simplifying plant operation, reducing construction times, and most importantly, enhancing the plant licensability [1]. The present study is being done for the Unconventional Trench-Type Sodium-Cooled Reactor, a research project sponsored by the U.S. Department of Energy, and currently being studied at the Department of Nuclear Engineering at Iowa State University [2].

The trench reactor is a long, narrow slab reactor with a long, narrow core which is located in a sodium pool. The pool is 21 meters long, 4 meters wide and 18 meters high. The reactor has an operating power of 800 MW (thermal). A detailed description of the trench reactor is given in Chapter 2.

The method of cooling by natural circulation, first suggested by Coffield et al [3] involves a passive cooling system, where the heat is rejected to the containment gas by

natural convection and radiation. This type of a system is inherently reliable and safe since it is free of the types of failures associated with active cooling systems. As mentioned above the trench reactor has a rectangular geometry with one narrow side and one very long side. A baffle is put between the reactor walls and biological shield at an appropriate distance from the reactor walls. This forms a channel between the reactor walls and the biological shield. The reactor walls being at higher temperature than the gas in the channel, the gas near the wall is heated and rises, and thus a natural convection flow sets in. Some heat is also transferred to the baffle by radiation since it is at a relatively cooler temperature than the reactor walls. The baffle in turn rejects this heat to the gas by convection.

The present study is aimed at calculating the amount of heat that can be removed using such a system, and calculating the outlet and average gas temperatures in the channel for the Trench Reactor geometry and similar cases. This information is used in studying the effect of natural convection and radiation on the transient behavior of reactor wall temperature. The physical situation is modeled as a three-part heat transfer: (1) convection from reactor walls to the gas, (2) radiation from reactor walls to the

baffle, and (3) convection from baffle to gas. After making a few simplifying assumptions about the flow conditions and operating conditions as indicated in Chapter 3, the heat transfer equations are formulated. Using a nodal method and an iterative scheme which is described in Chapter 3, these equations are programmed to perform the necessary computations. The program uses wall temperature, gas inlet temperature and convective and radiative properties as input parameters. The output of the program contains outlet gas temperature and the baffle temperature, both of which are guessed initially and found iteratively; as well as the total heat removal rate. The results of the sensitivity analysis for some of the important input variables are given in Chapter 4. Also presented in Chapter 4 is the change in reactor wall temperature, as well as baffle and gas outlet temperatures with time as a function of important input variables for the cases when there is no cooling and when there is cooling by natural convection.

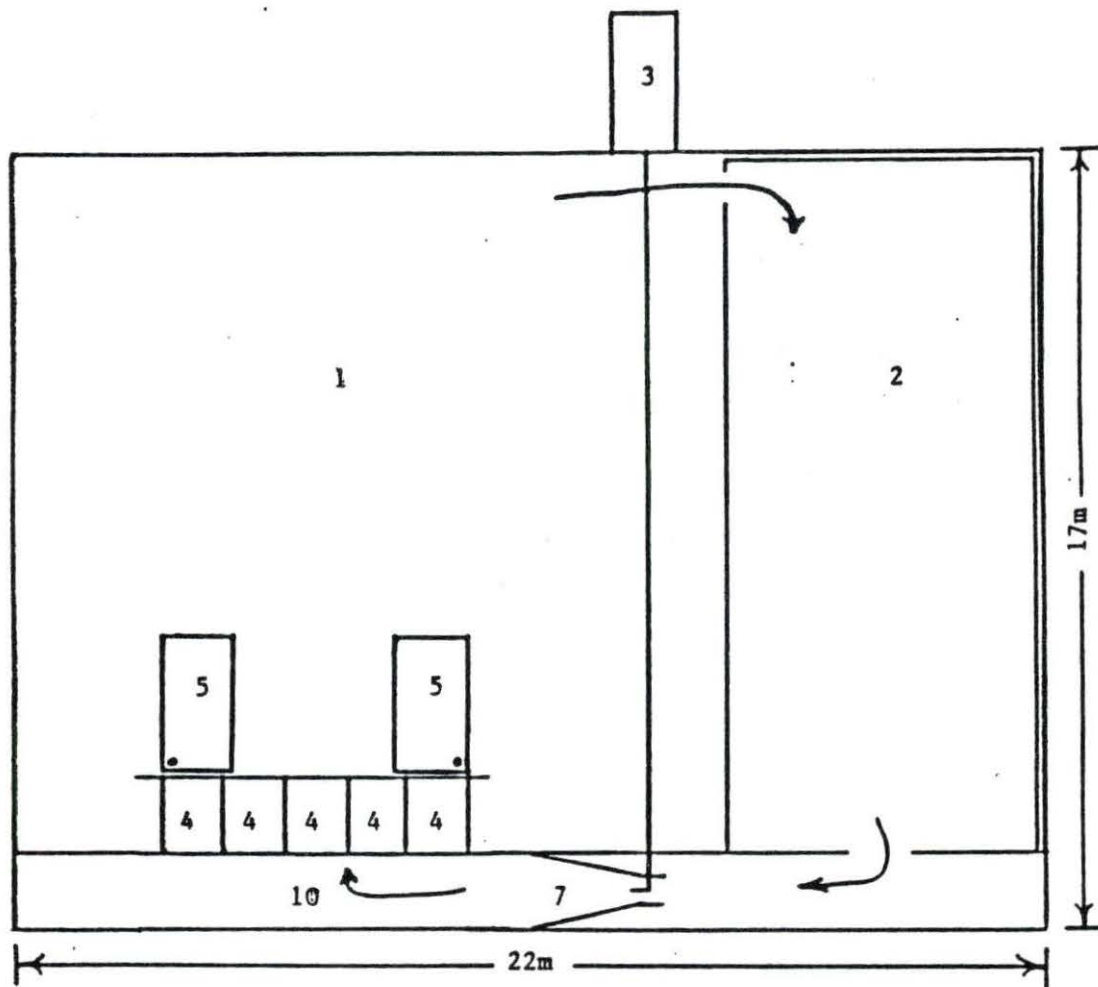
The calculations done in this study are basic and simple in nature because of the assumptions made in order to formulate and solve the heat transfer equations. Critical evaluation of this study as well as suggestions for further work are stated in Chapter 5.

2. DESCRIPTION OF THE SYSTEM

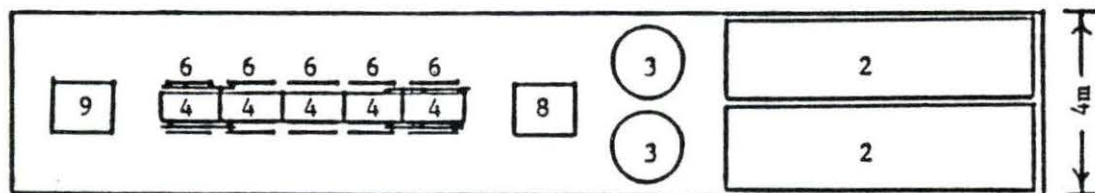
2.1 The Trench Reactor

The unconventional sodium cooled, trench type fast reactor concept was proposed in 1985 [2] and is currently being studied and developed at the Department of Nuclear Engineering at Iowa State University. The trench reactor is a fairly narrow, slab reactor; long in one horizontal dimension, located in a long, narrow sodium pool. The core has five integral boxes made of 1 cm. thick steel. The core has overall dimensions 0.65 meters (lateral) x 6.5 meters (longitudinal) x 1.5 meters (axial or vertical). The fuel is a metallic alloy of Uranium-Plutonium-Zirconium, and the cladding is HT-9 steel. Each box in the core has blankets on each side in the lateral direction and blankets and reflector plugs of steel in the axial direction. There is an upper plenum of about 2 meters and a lower plenum of about 3 meters in the core. The pool is 21 meters long and 4 meters wide with a total height of 18 meters. Fig. 1 shows two views of the trench reactor showing important components. The reactor has a nominal power of 800 MW(th).

- | | |
|--------------------|--------------------|
| 1. Sodium Pool | 6. Shim Elements |
| 2. Heat Exchangers | 7. Jet Pump |
| 3. Coolant Pumps | 8. Loading Table |
| 4. Core Modules | 9. Unloading Table |
| 5. Safety Elements | 10. Inlet Plenum |



(a) Vertical Section



(b) Horizontal Section

FIGURE 1. Cross Section Views of the Trench Reactor [7]

2.2 Decay Heat Produced in a Reactor

The decay heat produced in a nuclear reactor after shutdown is an important consideration in the design of the reactor. When a reactor is shut down, the accumulated fission products continue to decay and release energy within the reactor [4]. Judd [5] has mentioned that one second after shutdown in a Fast Breeder Reactor that has been operating for a very long time, the decay energy is about 6.2 percent of the reactor operating power and it decreases exponentially with time. This is a substantial amount of heat and it needs to be removed from the reactor. If the decay heat is not removed, the core would get overheated and the fuel temperatures would increase. This may lead to disintegration of fuel elements and subsequent release of fission products. Decay heat removal is necessary to restrict vessel temperatures to values compatible with containment structure sizing criteria and also to cool the system and hold it at low temperatures for servicing and handling operations [6]. Thus a reactor design must have sufficient cooling arrangement to cool the reactor after shutdown.

2.3 Shutdown Cooling of the Trench Reactor

The trench reactor has an operating power of 800 MW(th) as stated in Section 2.1. Preliminary studies have shown that natural circulation of coolant sodium through the core and a cooled intermediate heat exchanger (IHX) can effectively remove 56 MW of heat [7].

A rough calculation using an empirical formula from Broadley and McSweeney [8] shows that for a fast breeder reactor, at an hour after shutdown, about 11 MW of heat is produced in the trench reactor. It is of interest to know if the containment gas in the building can cool the reactor by removing this heat by free convection. It would also be important to know how the wall temperature changes with time when the reactor vessel walls are cooled by natural circulation of the containment gas, which will likely be nitrogen or some other inert gas. Air is not suitable for use as a containment gas because sodium reacts violently with air and this reaction would be hazardous in the event of a leak. Nitrogen is cheap and easily available commercially. It has good heat transfer properties. Therefore, it is one of the attractive candidates for use as containment gas.

2.4 Natural Circulation Loop

As stated in Chapter 1, a channel is formed by the baffle which is put at an appropriate distance from the reactor vessel outer walls. The baffle will most probably be steel plates forming an open box with no bottom or top which will be put between the reactor walls and the biological shield. This channel will henceforth be called the inner channel. A proposed mechanism to keep the inner channel closed to gas flow when the reactor is operating is by using a valve. After shutdown or under accident conditions, the valve is to be automatically opened. When the channel is open, the gas flows in the inner channel. The walls being at higher temperature than the gas, the gas near the walls is heated and thus rises.

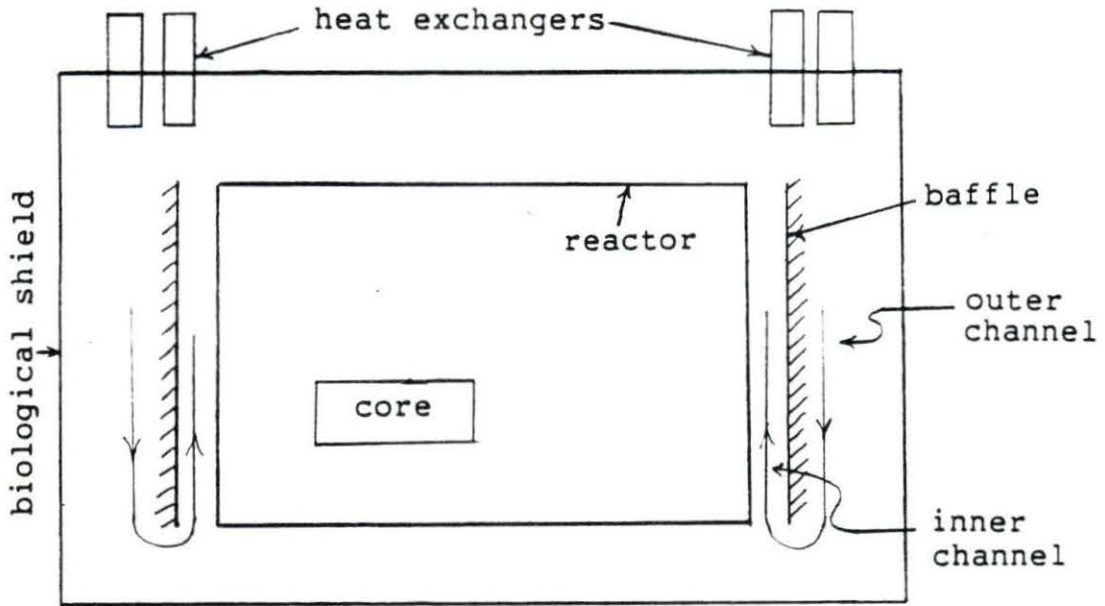
The reactor walls are at sufficiently high temperature (482.22°C or 900°F and higher) that radiation becomes a significant mode of heat transfer. Since the reactor walls are at higher temperature than the baffle, a net radiative heat transfer takes place from the walls to the baffle. The baffle rejects heat to the gas by natural convection. The gas in the inner channel is thus heated by both the reactor walls and the baffle.

As shown in Fig. 2, a channel is also formed between the baffle and the biological shield. This channel will be

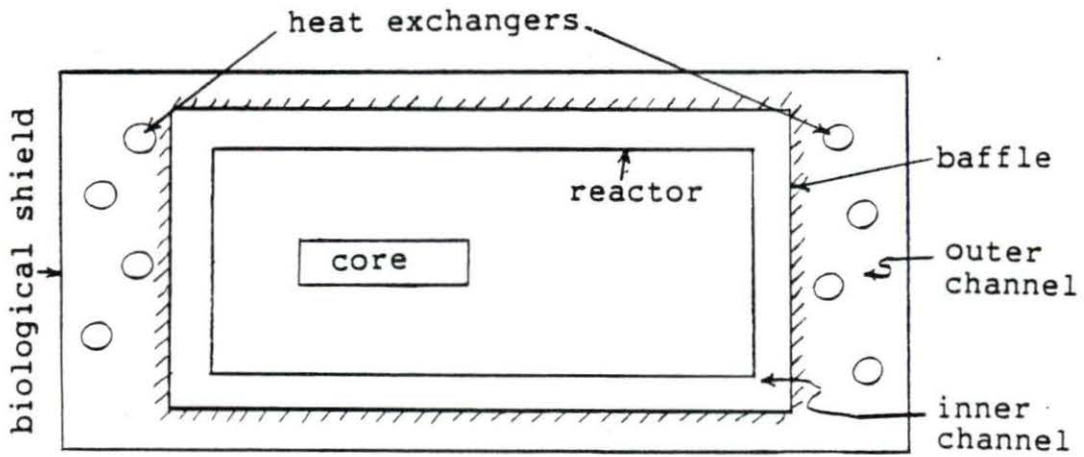
referred to as the outer channel. The side of the baffle facing the biological shield is insulated so that the baffle does not reject any heat to the gas in the outer channel. The gas in the outer channel is at a cooler temperature than the gas in the inner channel. The natural circulation loop consists of the heated gas rising in the inner channel, rejecting the heat at the containment top to a heat exchanger and the cool gas returned down the outer channel.

A heat exchange system is needed near the top of the containment building to reject heat from the containment gas to the atmosphere. A suggestion is to use a series of heat pipes with Freon or some other refrigerant as the fluid. These heat exchangers would go through the ceiling of the containment building and out into the atmosphere. The gas inside the containment building should be at a higher pressure than the atmospheric pressure so that in the event of a leak, the inside gas leaks out rather than the atmospheric air entering the building. As mentioned earlier, air reacts violently when it comes in contact with sodium. A reserve supply of the containment gas is needed to replenish the gas if it leaks out. A sensitive pressure sensor is needed so that a leak is detected promptly.

It is of interest to study the heat transfer characteristics of such a natural circulation loop and the



(a) Side view



(b) Top view

FIGURE 2. Schematic views of the Natural Circulation Loop

effect of cooling by natural convection and radiation on the transient behavior of reactor vessel walls. This study is a first attempt to model and solve the system by making appropriate approximations to make the problem manageable. The details of the method of solution are presented in Chapter 3.

3. METHOD OF SOLUTION

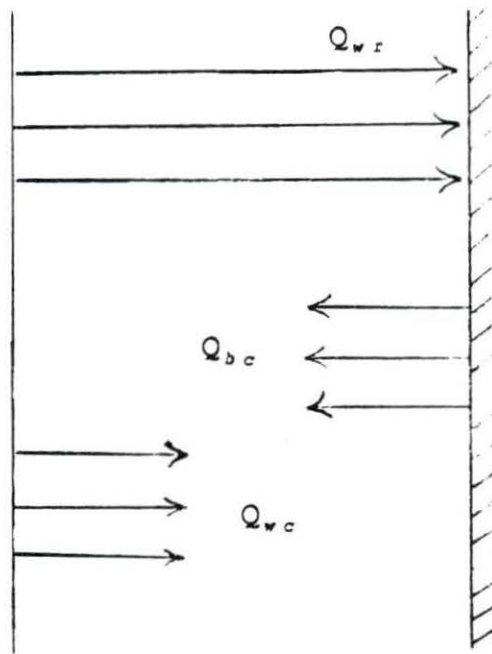
The objective of the present study is to calculate the amount of heat that can be removed by natural circulation of the containment gas in the trench reactor, and the effect of cooling on the transient behavior of the reactor wall temperature. In this chapter, the problem is stated first, followed by major assumptions used in the study. Finally, the method of solution including the equations used, is described.

3.1. The Problem

As mentioned in Chapter 1, the problem of heat transfer from the reactor walls to the containment gas by free convection is a three-part problem:

- Convective heat transferred from the reactor walls to the gas, Q_{wc}
- Radiative heat transferred from reactor walls to the baffle, Q_{wr}
- Convective heat transferred from baffle to the gas, Q_{bc}

This is also explained in Fig. 3. It should be noted that Q_{bc} and Q_{wr} are assumed to be equal, i.e., all the heat coming into the baffle by radiation is rejected to the gas by natural convection.



Q_{wc} - Convective heat transferred from the reactor walls to the gas

Q_{wr} - Radiative heat transferred from reactor walls to the baffle

Q_{bc} - Convective heat transferred from baffle to the gas,

FIGURE 3. Modes of Heat Transfer for the Inner Channel

3.2. Assumptions

An exact analysis of the combined free convection and radiation problem described above is very complex due to the coupling between convection and radiation heat transfer and also because the channel is formed by two walls at different temperatures.

In order to simplify the problem and make it more tractable, the following assumptions have been made:

- The gas flow is fully developed, and there is turbulent natural convection flow over most of the channel length (i.e., the entry length is small compared to the channel length of the inner channel).
- The velocity profile of the gas in the direction perpendicular to the walls and the baffle is symmetric, and is similar to the fully developed turbulent forced convection flow.
- The gas flow in the inner channel is considered a one dimensional flow along the vertical (axial) direction.
- The temperature of the reactor walls is uniform across the whole wall surface.
- The baffle is at a uniform temperature.

- The thermal conductivity and specific heat of the gas are independent with respect to temperature. However, the density and viscosity of the gas are temperature-dependent.
- The fraction of the total pressure drop at entrance-exit is assumed to be an empirical constant.
- The gas is flowing through the inner channel at a velocity found by equating buoyancy with the total pressure drop in the circuit.
- There is no unheated chimney section at the top of the inner channel.
- The baffle is insulated on the outer side. There is no heat transferred to the gas in the outer channel.
- All the heat entering by radiation from the walls is rejected by convection to the gas.
- The gas is transparent to radiation heat transfer, i.e., it acts as a nonparticipating medium.
- The surface roughness of the reactor walls and the baffle is similar to that of smooth pipes.

The first two are the most restricting assumptions, but they help simplify the analysis of the problem considerably. Calculations of the Raleigh number which are shown in

Appendix A indicate that the flow is turbulent for most of the inner channel. As mentioned earlier, the channel is formed by two walls at two different temperatures. The reactor walls are at a higher temperature than the baffle. As a result, the velocity profile of the gas will be non-symmetric with the peak shifted towards the reactor walls. For lack of better correlations for frictional pressure loss and Nusselt number for such conditions, the assumption of symmetric velocity profile has been made. This allows the use of available correlations for frictional pressure loss and heat transfer coefficient as stated in Section 3.3. In a recent study of a similar problem at the Argonne National Laboratory, similar assumptions have also been used [1].

Assuming a one dimensional flow makes formulation of the problem simpler. It has been used as a first approximation and would be extended to two and three dimensions in the future. For the present problem, the temperature variation in the horizontal direction is not expected to be much compared to the vertical direction. Therefore, a one-dimensional model would give useful information about the reactor wall temperature as a function of time. The assumption of uniform reactor wall temperature is reasonable. The high thermal conductivity of liquid metal would imply that the pool is at a uniform temperature

and also that the reactor walls are at a uniform temperature. The baffle temperature has been assumed uniform to simplify the problem. Variation in baffle temperature can be handled without adding too much complexity as far as the computer programming is concerned.

The assumption of constant thermal conductivity and specific heat is not very erroneous. Both properties are fairly constant over the range of temperatures involved in this study and vary by less than 1 percent. However, considering these properties temperature-dependent will not be very difficult in the present model.

The assumption about entrance-exit pressure loss makes the results necessarily parametric rather than specific. A more detailed analysis needs to be performed to calculate the true entrance-exit pressure loss for the flow conditions in this study. The velocity found by equating buoyancy with the total pressure drop in the circuit is strongly dependent on the pressure drop at the entrance-exit. Therefore, the assumption that the gas flows at this velocity also becomes restricting.

Assuming that there is no chimney section on top of the inner channel makes the problem simple to model and solve. However, this is a first approximation and also a conservative assumption. Study of the effect of a chimney

on the heat transfer and sensitivity analysis for the chimney height should be done in the future. It is expected that addition of chimney would enhance the heat transfer. But it would be costly as well as inconvenient to have large chimney heights.

The baffle plate could be easily insulated on one side. Thus, the assumption about the baffle being insulated on the side facing the containment building is fairly correct. The assumption that all heat coming into the baffle is rejected to the gas is made to treat the transient problem of change in reactor wall temperature as a series of steady states. The assumption of the gas being transparent to radiation heat transfer is also reasonable since nitrogen and other inert gases are indeed transparent to radiation.

The assumption that the surface roughness of the reactor walls and the baffle is similar to that of smooth pipes is a reasonable approximation since the surface roughness index would be much lower than the dimensions of the inner channel. On one hand, the surface roughness would mean an increase in area and would act as turbulence promoter, resulting in better heat transfer. But on the other hand, it would also increase the frictional pressure loss, causing lower mass flow rate and less heat transfer. The surface emissivity is an important parameter that

affects the radiation heat transfer. Therefore, the effect of different types of surfaces on heat transfer should be studied in the future and the surface that gives the best performance can be used for design purposes.

3.3 Method of Solution and Governing Equations

Using the approximations stated in Section 3.2, the transient heat transfer equation is:

$$M_{Na} C_{pNa} \frac{dT_w}{d\theta} = 0.134P_o \theta^{-0.285} - UA_w(T_w - T_g) \quad (3.1)$$

where the term on the left hand side is the heat accumulation in the pool; M_{Na} is the mass of the sodium in the pool, C_{pNa} is the specific heat of sodium, θ is the time after shutdown in seconds, T_w is the wall temperature which is assumed to be the same as the pool temperature of sodium and T_g is the average temperature of the gas in the channel.

The first term on the right hand side is a semi-empirical formula for the decay heat production for Liquid-Metal cooled Fast Breeder Reactors (LMFBRs) for large fuel burn-ups. The correlation is valid for times after shutdown between 1 and 300,000 seconds. P_o is the full thermal output of the reactor [8]. A comparison of this correlation with tabulated data for different times after shutdown is presented in Appendix B. It must be mentioned, however,

that this correlation might be somewhat different for the trench reactor and this would change the results of the present analysis accordingly. The advantage of using this correlation is that it is easier to incorporate in the analysis. It is good for a first approximation similar to other assumptions made in the present study.

The second term on the right hand side is the heat loss term. U is the overall heat transfer coefficient which accounts for convective and radiative heat loss from the reactor walls. A_w is the surface area of the reactor walls, which is given by

$$A_w = 2(L + W)H \quad (3.2)$$

where L is the length of the reactor vessel, W is the width of the reactor vessel and H is the height of sodium level in the pool. T_g is the average temperature of the gas in the channel.

The differential equation (3.1) is solved numerically to compute the wall temperature as a function of time. The heat generation term in equation (3.1) changes slowly with time, whereas the heat loss term changes rapidly with time. The heat loss term has been calculated for constant T_w and used in the present model.

The heat loss term on the right hand side is not simple to calculate since the heat transfer coefficient for the situation in this problem is not available. Using the first two approximations stated in Section 3.2, the Sieder-Tate correlation can be used to calculate the heat transfer coefficient. This correlation is a modified form of the Dittus-Boelter correlation for fully developed, turbulent forced convection flow in a uniformly heated tube. The convective heat transferred from the reactor walls to the gas is given by

$$Q_{wc} = hA_w(T_w - T_g) \quad (3.3)$$

where h is the heat transfer coefficient given by the Sieder-Tate correlation [9].

$$h = 0.02 \left(\frac{K}{H} \right) \text{Re}^{0.8} \left(\frac{\mu_{gav}}{\mu_{gw}} \right)^{0.14} \quad (3.4)$$

where K is the thermal conductivity of the gas, Re is the Reynolds number, μ_{gav} and μ_{gw} are the viscosities of the gas at average channel gas temperature and wall temperature respectively.

The radiative heat transferred from the reactor walls to the baffle is given by

$$Q_{wr} = \frac{F_{wb} \sigma A_w (T_w^4 - T_b^4)}{\left(\frac{2}{\epsilon} - 1 \right)} \quad (3.5)$$

where F_{wb} is the view factor between the walls and the baffle. The formula for the view factor was used for two finite parallel plates [10]. This formula is given in Appendix C. σ is Stefan-Boltzmann's constant, ϵ is the emissivity which is assumed to be the same for the reactor walls and the baffle, and T_b is the baffle temperature.

The equation for convective heat transfer from the baffle to the gas is similar to equation (3.3)

$$Q_{bc} = hA_b(T_b - T_g) \quad (3.6)$$

where A_b is the total area of the baffle surface facing the inner channel.

The assumption that the radiative heat coming into the baffle from the reactor walls is rejected to the gas by convection implies that equations (3.5) and (3.6) can be equated as follows

$$\frac{F_{wb}\sigma A_w(T_w^4 - T_b^4)}{\left(\frac{2}{\epsilon} - 1\right)} = hA_b(T_b - T_g) \quad (3.7)$$

The total amount of heat picked up by the gas is obtained by adding equations (3.3) and (3.6). This is equal to the heat rejected by the reactor walls and the baffle to the gas in the inner channel. This can be written as

$$\begin{aligned} hA_w(T_w - T_g) + hA_b(T_b - T_g) \\ = m_g C_{p_g}(T_{g_o} - T_{g_i}) \end{aligned} \quad (3.8)$$

where m_g is the mass flow rate of the gas, C_{p_g} is the specific heat of the gas; T_{g_i} and T_{g_o} are the gas temperatures at the inlet and outlet, respectively, of the inner channel.

In equation (3.8), there are three unknowns namely T_b , m_g and T_{g_o} . These three variables are interdependent, i.e., m_g depends on T_{g_o} and T_{g_o} is in turn determined by m_g as well as T_b . In the present study, an iterative procedure is employed using a finite difference technique by dividing the inner channel into a number of nodes of equal height. The method of solution and the governing equations are described below.

3.3.1 Iterative procedure and nodal method

The inner channel is divided into a number of nodes as shown in Fig. 4. The iterative procedure used involves iterating upon T_b and T_{g_o} as follows:

1. Guess a value of baffle temperature, T_{b_g} .
2. Guess a value of channel outlet temperature for the containment gas, T_{g_o} .
3. Find density of the gas corresponding to T_{g_o} , ρ_{g_o} .

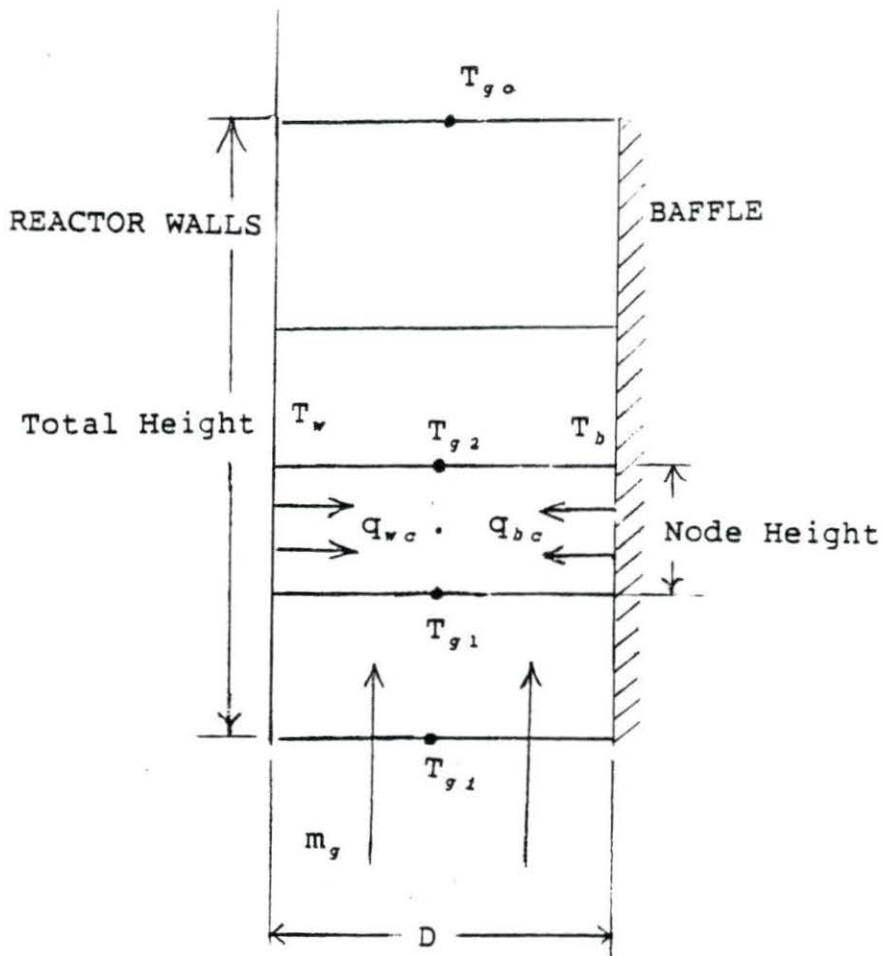


FIGURE 4. Nodal Representation of the Inner Channel

4. Calculate v_{av} , average velocity in the inner channel by equating buoyancy with total pressure drop. The total pressure drop Δp_{tot} is given by

$$\Delta p_{tot} = \Delta p_{ee} + \Delta p_{fric} \quad (3.9)$$

where Δp_{ee} is the pressure drop at entrance-exit. The approximation that the entrance-exit pressure drop is an empirical fraction of the total pressure drop implies that

$$\Delta p_{ee} = \Omega \Delta p_{tot} \quad (3.10)$$

where Ω is the ratio of the pressure drop at entrance-exit to the total pressure drop and is assumed to be a number between 0.4 and 0.8 [1].

Δp_{fric} is the frictional pressure drop given by [10]

$$\Delta p_{fric} = 4fH \frac{\rho_{gav} v_{av}^2}{D_e} \quad (3.11)$$

In equation (3.11), H is the height of the inner channel, D_e is the equivalent diameter, ρ_{gav} is the average density in the inner channel which is given by

$$\rho_{gav} = 0.5(\rho_{g1} + \rho_{g0}) \quad (3.12)$$

and f is the friction factor which can be written for fully developed turbulent flow and for surface of smooth pipes as follows [10]

$$f = 0.079\text{Re}^{-0.25} \quad (3.13)$$

Substituting f from equation (3.13) in equation (3.11) and putting equation (3.11) and equation (3.10) in equation (3.9), total pressure drop can be expressed as

$$\Delta p_{tot} = \frac{0.158}{(1-\Omega)} \frac{H}{D_e} \left(\frac{D_e}{\mu_{g_{av}}} \right)^{0.25} (\rho_{g_{av}}^{0.75}) (v_{av}^{1.75}) \quad (3.14)$$

The buoyancy term can be written as [10]

$$\Delta p_b = 0.5(\rho_{g_i} - \rho_{g_o})gH \quad (3.15)$$

where ρ_{g_i} and ρ_{g_o} are the densities of the gas corresponding to the channel inlet and the channel outlet temperature respectively and g is the gravitational acceleration.

Thus, the average velocity is calculated as follows

$$v_{av} = \left(\frac{\text{Num}}{\text{Den}} \right)^{0.5714} \quad (3.16)$$

$$f(x) = \frac{1}{x^2}$$

$$f'(x) = -\frac{2}{x^3}$$

$$f''(x) = \frac{6}{x^4}$$

$$\frac{\delta}{x} = \frac{4.92}{\sqrt{\frac{u_{\infty} x}{\nu}}} \rightarrow \sqrt{\frac{u_{\infty}}{\nu x}} = \frac{4.92}{\delta(x)}$$

$$\frac{u}{u_{\infty}} = f(\eta)$$

$$f' \left(\frac{y}{\sqrt{\frac{\nu x}{u_{\infty}}}} \right)$$

where Num and Den are defined as follows

$$\text{Num} = 0.5(\rho_{g_i} - \rho_{g_o})gH \quad (3.17)$$

$$\text{Den} = \frac{0.158}{(1-\Omega)} \frac{H}{D_e} \left(\frac{D_e}{\mu_{g_{av}}} \right)^{0.25} (\rho_{g_{av}}^{0.75}) \quad (3.18)$$

5. Calculate the mass flow rate of the gas m_g using

$$m_g = v_{av} \rho_{g_{av}} A_f \quad (3.19)$$

where v_{av} is the average velocity obtained from equation (3.16), and A_f is the cross sectional flow area which is given for the rectangular annulus by

$$A_f = (L + W + D_e)D_e \quad (3.20)$$

where L is the length of the reactor vessel, W is the width of the reactor vessel and D_e is the equivalent diameter which is given for the trench reactor geometry by

$$D_e = 2D \quad (3.21)$$

where D is the distance between the reactor walls and the baffle.

6. For the first node, the inlet temperature to the inner channel is the inlet temperature for the node.
7. Knowing inlet temperature to a node, T_{g1} , the density ρ_{g1} and viscosity μ_{g1} corresponding to T_{g1} are calculated. The velocity for the node, v_{node} is found by using

$$v_{node} = \frac{m_g}{\rho_{g1} A_f} \quad (3.22)$$

Then, the Reynolds number is calculated as follows

$$Re = \frac{D_e v_{node} \rho_{g1}}{\mu_{g1}} \quad (3.23)$$

8. The heat transfer coefficient for the node, h_{node} is calculated using the Sieder-Tate correlation

$$h_{node} = 0.02 \left(\frac{K}{H} \right) Re^{0.8} \left(\frac{\mu_{g1}}{\mu_{gw}} \right)^{0.14} \quad (3.24)$$

9. The total heat transferred to the gas for a node is the sum of convective heat transferred from the reactor walls to the gas given by equation (3.25), and the convective heat transferred from the baffle to the gas given by equation (3.26)

$$q_{nw} = h_{node} A_{nw} (T_w - T_{g1}) \quad (3.25)$$

$$q_{nb} = h_{node} A_{nb} (T_b - T_{g1}) \quad (3.26)$$

A_{nw} and A_{nb} are the areas of each node for the reactor walls and the baffle given by equation (3.28) and (3.29), respectively. It should be noted that the values of density ρ_{g1} and viscosity μ_{g1} used in the calculation of heat transfer coefficient h_{node} are taken corresponding to the inlet temperature of the gas for the node rather than the average temperature for the node. To calculate q_{nw} and q_{nb} , the inlet temperature to the node is used instead of the average temperature for the node, T_{gnode} given by

$$T_{gnode} = 0.5(T_{g1} + T_{g2}) \quad (3.27)$$

However, since T_{g2} is unknown, an iterative procedure would have to be used. This would involve guessing a value of T_{g2} , then finding properties at the average temperature for the node, calculating the heat transfer coefficient, calculating the heat transferred for the node and finally calculating T_{g2} from equation (3.31).

The iteration can be continued by checking for convergence between the guessed value of T_{g_2} and calculated value of T_{g_2} and redefining the guessed value until the desired convergence criterion is satisfied. This procedure would need more computations and for a node size for which there is not a very large difference between the inlet and outlet temperatures for the node, it does not contribute significantly to the accuracy of the results. Therefore, T_{g_1} has been used in the present study instead of $T_{g_{node}}$.

A_{nw} and A_{nb} are the areas of each node for the reactor walls and the baffle given by equation (3.28) and (3.29), respectively.

$$A_{nw} = 2(L + W)\Delta H \quad (3.28)$$

$$A_{nb} = 2(L + W + D_e)\Delta H \quad (3.29)$$

where ΔH is the height of each node.

Thus, total heat transferred for the node q_{node} is given by

$$q_{node} = q_{nw} + q_{nb} \quad (3.30)$$

10. The outlet temperature of the gas for a node T_{g_2} is found by equating the total heat transferred to the gas with the increase in the enthalpy of the gas. Thus, T_{g_2} is given by

$$T_{g_2} = T_{g_1} + \frac{Q_{node}}{m_g C_{p_g}} \quad (3.31)$$

11. The outlet temperature for a node is the inlet temperature for the next node. Using this, steps 7 through 10 are repeated through the last node at the top of the inner channel.
12. The outlet temperature for the last node T_{g_f} is compared with the guessed value of the channel outlet temperature T_{g_o} . The term ϵ_g defined by equation (3.32) is the measure of how close the calculated value of channel outlet temperature is to the guess value.

$$\epsilon_g = \left| \frac{T_{g_o} - T_{g_f}}{T_{g_o}} \right| \quad (3.32)$$

The convergence parameter for ϵ_g was taken as 0.001 since it provided adequate accuracy and did not require too many iterations. If ϵ_g is greater than or equal to 0.001, the guessed value

of the channel outlet temperature T_{g_o} is reassigned as the calculated value T_{g_f} . Then, the steps 3 through 12 are repeated until the desired convergence has been obtained.

13. The iteration for the baffle temperature is done by equating the total radiative heat transfer from the reactor walls to the baffle to the total convective heat transfer from the baffle to the gas. Equation (3.7) is rewritten as follows

$$\frac{F_{wb} \sigma A_w (T_w^4 - T_{b_{old}}^4)}{\left(\frac{2}{\epsilon} - 1\right)} = hA_b (T_{b_{new}} - T_g) \quad (3.33)$$

The iteration is done as follows. $T_{b_{old}}$ is taken as the guessed value of the baffle temperature. The left hand side of equation (3.33) is then calculated. Using the value obtained thus, the value of $T_{b_{new}}$ is calculated. To check how close $T_{b_{new}}$ is to $T_{b_{old}}$, an error term ϵ_{be} is defined as follows

$$\epsilon_{be} = \left| \frac{T_{b_{old}} - T_{b_{new}}}{T_{b_{old}}} \right| \quad (3.34)$$

For ϵ_{be} less than or equal to 0.01, the value of baffle temperature is assumed to have

converged. The value of 0.01 was chosen for reasons similar to those mentioned for ϵ_g . If convergence has not been achieved, $T_{b_{old}}$ is redefined as follows

$$T_{b_{old}} = T_{b_{old}} + X(T_{b_{new}} - T_{b_{old}}) \quad (3.35)$$

where X is the relaxation parameter taken as 0.1. This value of relaxation parameter helped convergence for all the cases studied. The redefined value of $T_{b_{old}}$ is used in equation (3.33). The procedure is continued until the necessary convergence is achieved.

14. The iterated value of the baffle temperature T_{b_i} is compared with the guess value of the baffle temperature T_{b_g} . The error term ϵ_{b_o} is defined as

$$\epsilon_{b_o} = \left| \frac{T_{b_g} - T_{b_i}}{T_{b_g}} \right| \quad (3.36)$$

If ϵ_{b_o} is greater than or equal to 0.01, the guess value of the baffle temperature is redefined as

$$T_{b_g} = T_{b_g} + Y(T_{b_i} - T_{b_g}) \quad (3.37)$$

where Y is the relaxation parameter taken to be 0.1 for reasons similar to choosing 0.1 for X .

Steps 2 through 14 are repeated until the convergence of ϵ_{b_o} has been achieved.

As seen in steps 1 through 14, the iterative procedure involves iterating on two variables, the baffle temperature T_b and the channel outlet gas temperature T_{g_o} . The iteration criteria are stated for the baffle temperature in step 14, and for channel outlet gas temperature in step 12. Iteration has also been used to calculate a new value of baffle temperature given an old baffle temperature by equating radiative and convective heat transfer terms as described in step 13. However, this iteration is used as a method of solving equation (3.33). This is a fourth power equation which if solved exactly would yield 4 solutions and the method would be required to choose one and discard the rest which is more difficult to program into a computer. The iteration method used here gives fairly accurate results.

3.3.2 Transient behavior of wall temperature

The iterative procedure described above in Section 3.3.1 is used to calculate the total heat removal rate as a function of reactor wall temperature for different values of

other important variables. To study the effect of one variable, e.g., ϵ , the values of other variables, i.e., D , Ω , and $T_{g,i}$ are kept unchanged. The total heat removal rate is calculated as a function of wall temperature for different values of emissivity. The results are used to derive equations for heat removal rate as a function of wall temperature. This function is used as the heat loss term in equation (3.1) and the differential equation is solved using a computer program which uses a subroutine LSODA from the library ODEPACK on NAS AS/9160 computing system at Iowa State University. Equation (3.1) is rewritten below in the form in which it is solved

$$M_{Na} C_{pNa} \frac{dT_w}{d\theta} = 0.134 P_o \theta^{-0.285} - f(T_w) \quad (3.38)$$

The initial condition (I.C.) used is stated below

$$\begin{aligned} \text{I.C. : At time } \theta = 1 \text{ sec, } T_w &= 482.22^\circ \text{ C} \\ &= 900^\circ \text{ F} \end{aligned}$$

The subroutine computes the values of the reactor wall temperature T_w at different times specified in the program. The limiting case when there is no cooling is simulated by replacing $f(T_w)$ by 0 in equation (3.38).

The results of the computations are used to make plots of reactor wall temperature versus time, baffle temperature

versus time and channel outlet temperature of the gas versus time.

The programs to perform the tasks described in Sections 3.3.1 and 3.3.2 are listed in Appendices D and E, respectively.

4. RESULTS AND DISCUSSION

The results of the computations performed using the method of solution described in Chapter 3 are summarized in this Chapter. The results have been presented in two sections. The first section contains the results of computations performed using the iterative procedure and the nodal method. The procedure has been programmed to do the necessary calculations. The program takes as input variables the distance between the reactor walls and the baffle (D), the reactor wall temperature (T_w), the inlet gas temperature for the inner channel ($T_{g,i}$), and the values of the ratio of pressure drop at entrance-exit to total pressure drop (Ω) and emissivity (ϵ). The output of the program includes the total heat removal rate ($Q_{t.o.t}$), the channel outlet and channel average temperatures ($T_{g,o}$ and $T_{g,av}$ respectively), and the iterated value of the baffle temperature (T_b). The results have been presented in the form of families of plots. Each plot has an output variable, e.g., T_b , plotted as a function of T_w for different values of one of the other input variable, e.g., ϵ . The points denoted on the plots do not necessarily indicate calculated points, but are put to differentiate between the plots.

The second section contains the results of the computations which have been performed to study the transient behavior of T_w . These results have also been presented as families of plots. The variables plotted as a function of time are T_w , T_b and T_{g_o} . The limiting case of no cooling is also included in each plot.

The numerical values of the independent and dependent variables that have been used to make the plots have also been presented as tables in Appendices F and G.

4.1 Results of the Iterative Procedure

The procedure was followed for the inner channel by dividing the channel into 18 nodes, each node of height one meter. The reactor wall temperature was varied from 482.22°C (900°F) to 537.78°C (1000°F), the value of ϵ was taken from 0.6 to 1.0, the value of Ω was taken from 0.4 to 0.8, D was varied between 0.3048 m (1.0 ft) and 0.9134 m (3.0 ft), and T_{g_i} was varied between 37.78°C (100.0°F) and 71.11°C (160.0°F).

4.1.1 Total heat removal rate as a function of reactor wall temperature

For all the cases studied here, $Q_{t.o.t}$ increases with T_w , which is to be expected since with an increase in the wall

temperature, the amount of heat rejected to the gas would also increase. Fig. 5 shows $Q_{t \circ t}$ as a function of T_w with D as the other independent variable. As seen from the Fig. 5, $Q_{t \circ t}$ increases with an increase in D . However, this effect is obtained assuming that the value of Ω is the same for all the values of the distance used. It is expected that the value of Ω will change as D is varied. This would have an effect on the results obtained using this kind of an analysis. As D increases, the cross-sectional flow area increases, and the average velocity increases. This would account for the increase in $Q_{t \circ t}$.

Fig. 6 shows $Q_{t \circ t}$ as a function of T_w with ϵ as the other independent variable. With increase in ϵ , $Q_{t \circ t}$ also increases. Higher ϵ would mean that more heat would be transferred by radiation from the reactor walls to the baffle and the baffle then would reject this heat to the gas. ϵ equal to 1.0 is the case of a black wall which is difficult to achieve for real surfaces. However, a value of 0.7 and higher would provide an adequate heat removal rate for the system being studied here.

The effect of Ω on $Q_{t \circ t}$ as a function of T_w is shown in Fig. 7. $Q_{t \circ t}$ decreases with an increase in Ω . As Ω increases, the resistance to the flow in the inner channel increases. The average velocity as well as the mass flow

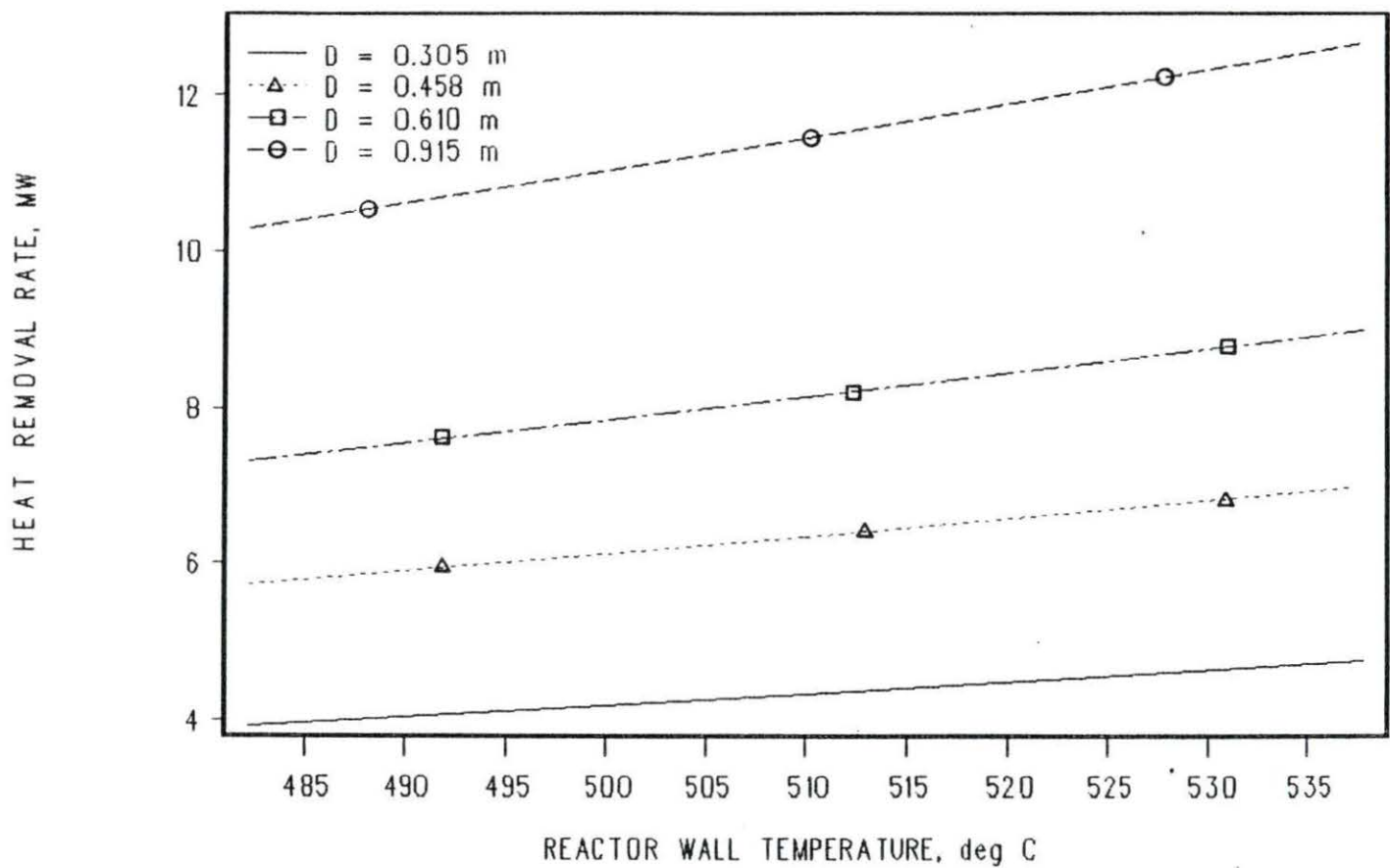


FIGURE 5. Total Heat Removal Rate versus Wall Temperature for different values D , with $\epsilon = 0.7$, $\Omega = 0.5$ and $T_{s,i} = 37.78^\circ \text{C}$

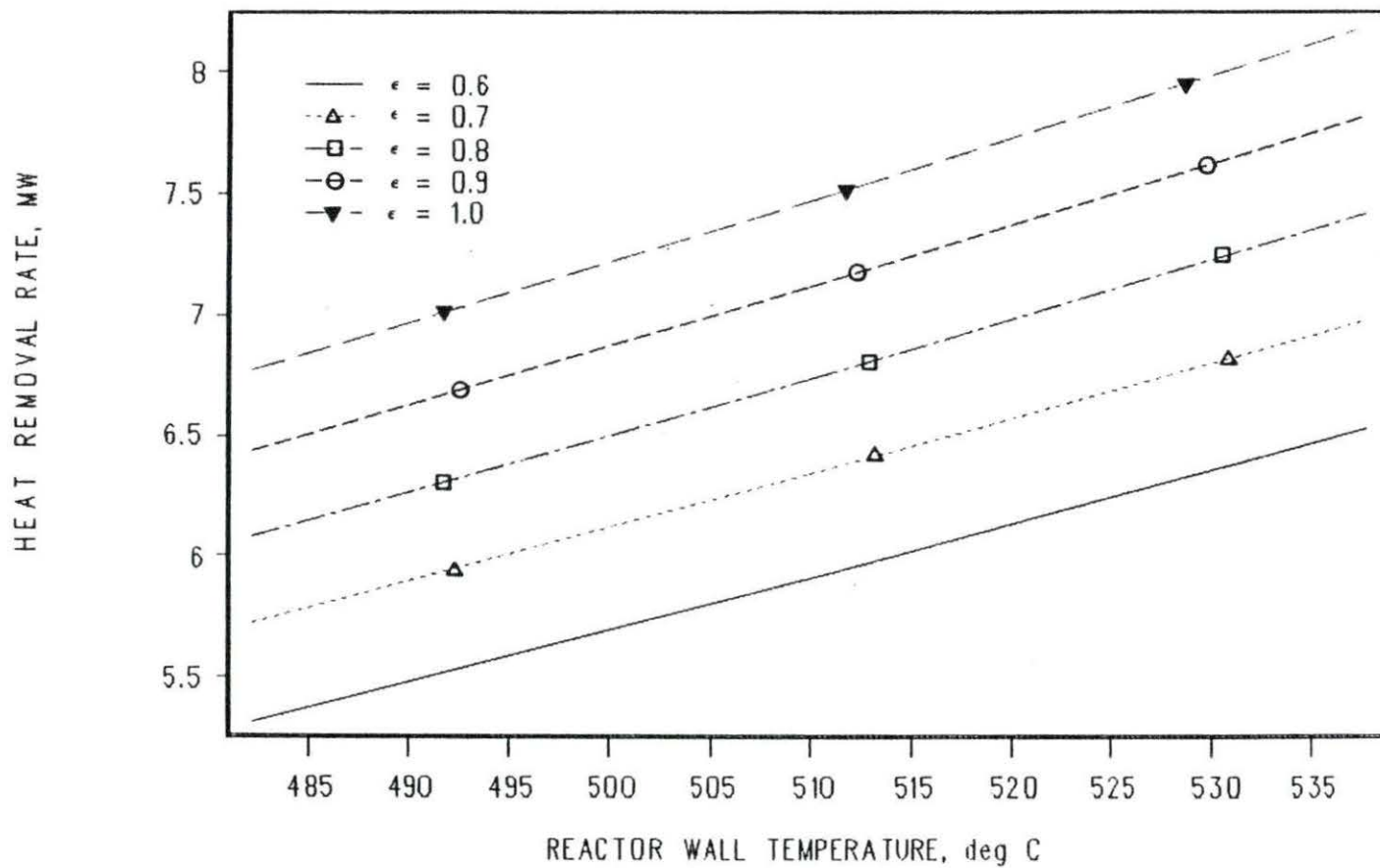


FIGURE 6. Total Heat Removal Rate versus Wall Temperature for different values of ϵ , with $D = 1.5$ ft, $\Omega = 0.5$ and $T_{s_1} = 37.78^\circ \text{C}$

rate in the inner channel decreases. Therefore, $Q_{t \circ t}$ decreases. This indicates that the inner channel should be designed such that the value of Ω is small.

Fig. 8 shows the effect of $T_{g,i}$ on $Q_{t \circ t}$ as a function of T_w . As $T_{g,i}$ increases, $Q_{t \circ t}$ decreases. The reason for this is that as the gas gets hotter, its ability to remove heat decreases since the temperature difference between the walls and the gas decreases. As seen in Fig. 8, for an increase of about 10°C in inlet temperature, there is a decrease of about 0.5 MW in $Q_{t \circ t}$.

4.1.2 Baffle temperature as a function of reactor wall temperature

The dependency of T_b on the T_w is linear for all the values of parameters used in the present study. T_b increases with increase in T_w as is expected since for higher values of T_w , more heat is transferred to the baffle by radiation results in a higher T_b . The variation in T_b with T_w for various values of other variables is presented in this section. Fig. 9 shows the plots of T_b versus T_w for different values of D . As D increases, the velocity and mass flow rate increase. Thus, there is better cooling resulting in lower values of T_b .

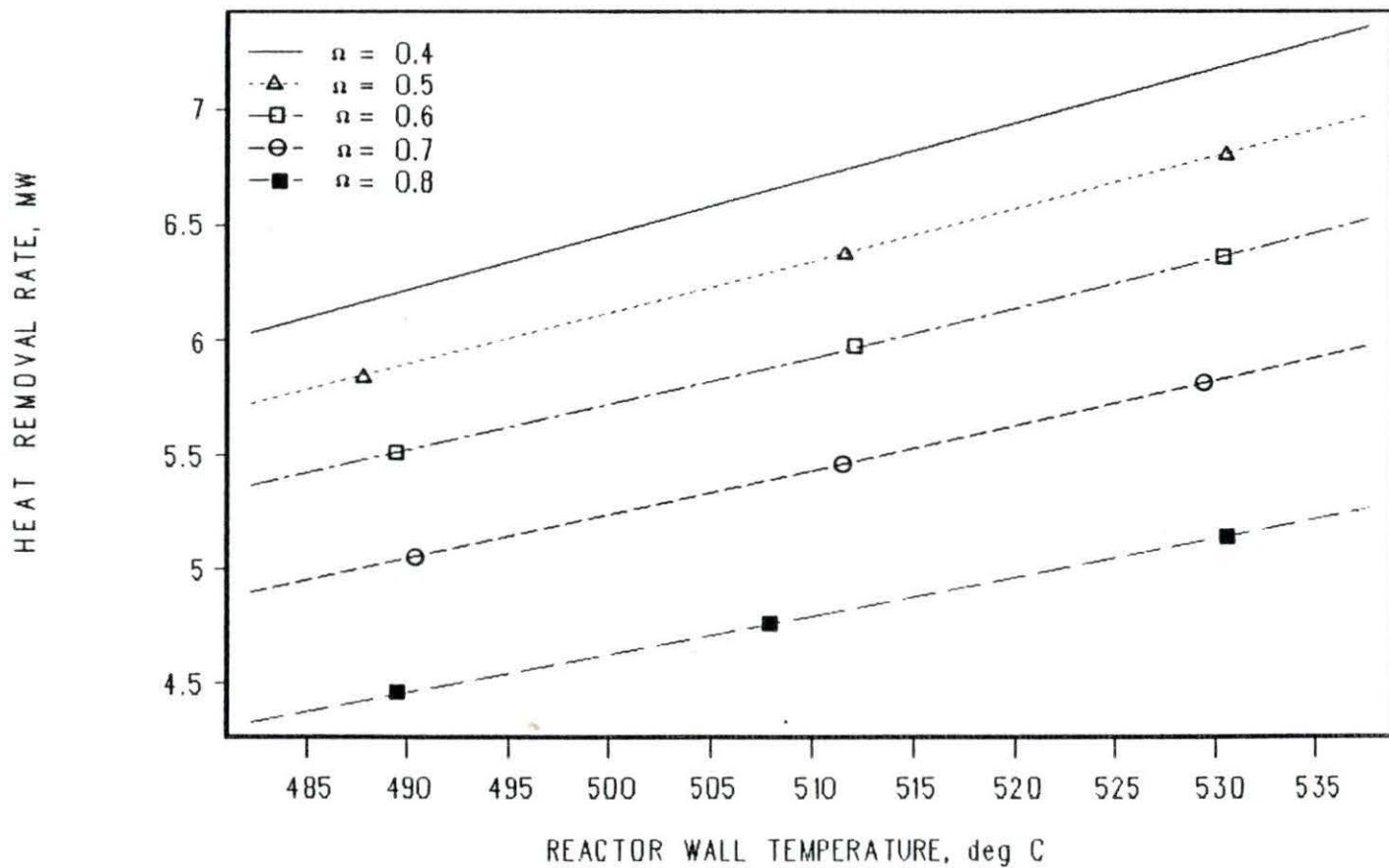


FIGURE 7. Total Heat Removal Rate versus Wall Temperature for different values of Ω , with $D = 1.5$ ft, $\epsilon = 0.7$ and $T_{s1} = 37.78^\circ \text{C}$

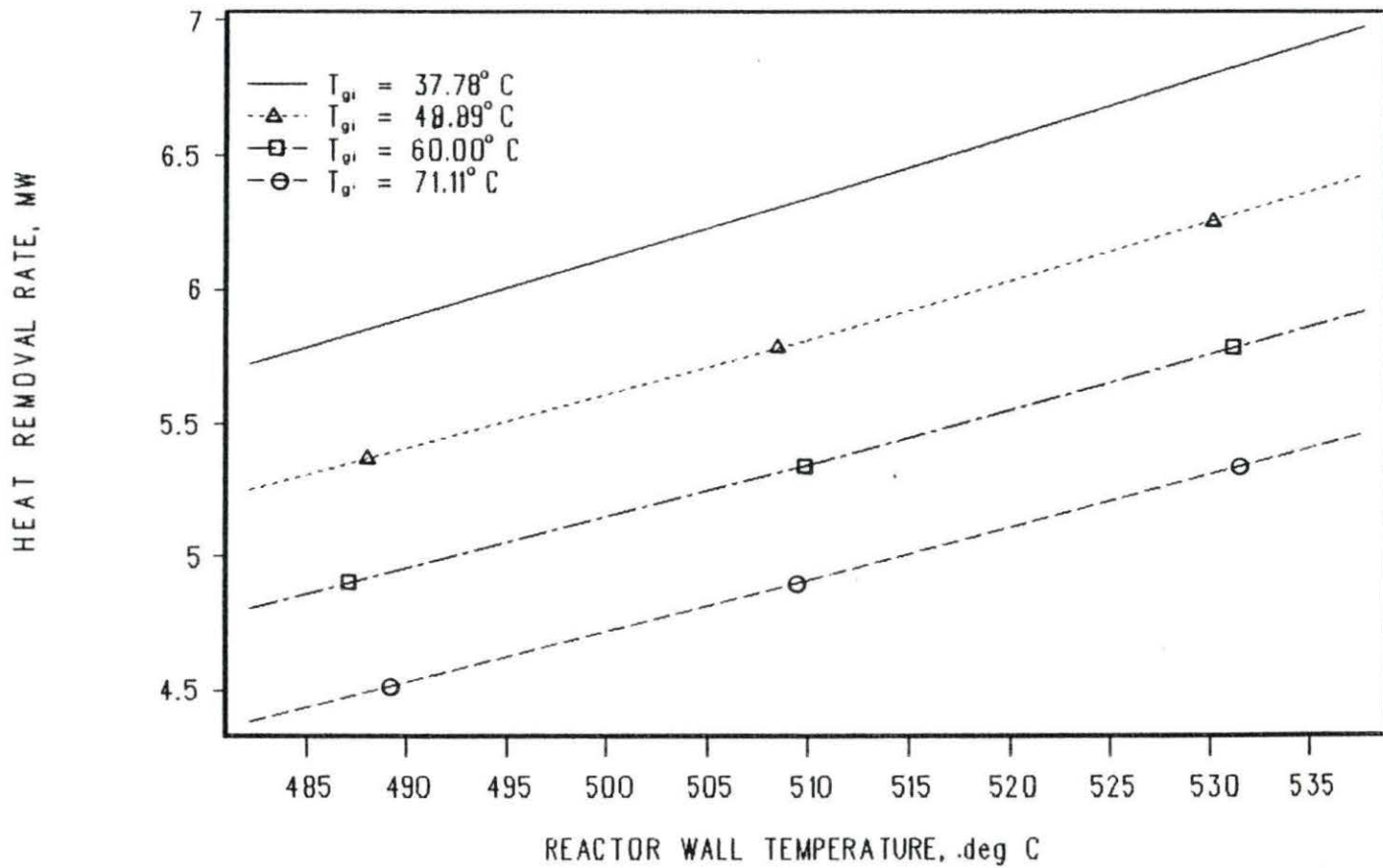


FIGURE 8. Total Heat Removal Rate versus Wall Temperature for different values of T_{g1} , with $D = 1.5$ ft, $\epsilon = 0.7$ and $\Omega = 0.5$

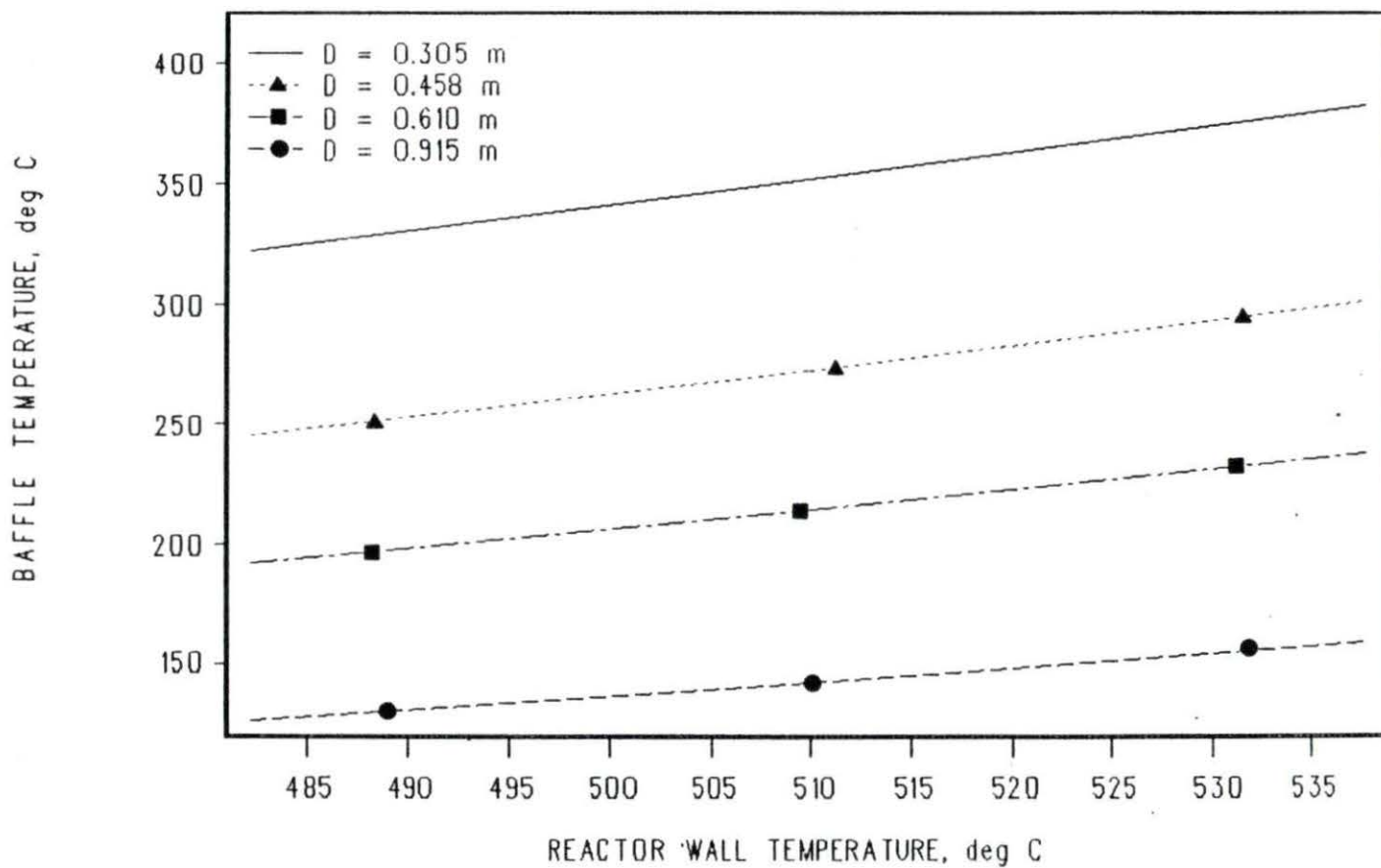


FIGURE 9. Baffle Temperature versus Wall Temperature for different values of D , with $\epsilon = 0.7$, $\Omega = 0.5$ and $T_{s,1} = 37.78^\circ \text{C}$

Fig. 10 shows plots of T_b versus T_w with the other independent variable as the ϵ . The T_b increases with increase in ϵ since the higher the ϵ , there will be more radiative heat transfer from the walls to the baffle and subsequently T_b would be higher.

The effect of Ω on the T_b as a function of T_w is shown in Fig. 11. It can be seen from the Fig. 11 that as Ω increases, T_b increases for the same value of T_w . For a higher value of Ω , there is more resistance to the gas flow resulting in lower flow rates. Therefore, the rate of heat removal by the gas is less. This will cause T_b to be higher.

Fig. 12 shows the effect of $T_{g,i}$ on T_b as a function of T_w . It was seen in section 4.1 that with an increase in the value of $T_{g,i}$, $Q_{t.o.t}$ decreases. Thus, there is less heat rejected to the gas. This causes the baffle temperature to increase.

4.1.3 Channel outlet gas temperature as a function of wall temperature

The plots presented in this section indicate that $T_{g,o}$ changes very slowly with the T_w . Fig. 13 shows $T_{g,o}$ as a function of T_w for different values of D . $T_{g,o}$ increases linearly with the T_w which is to be expected since higher

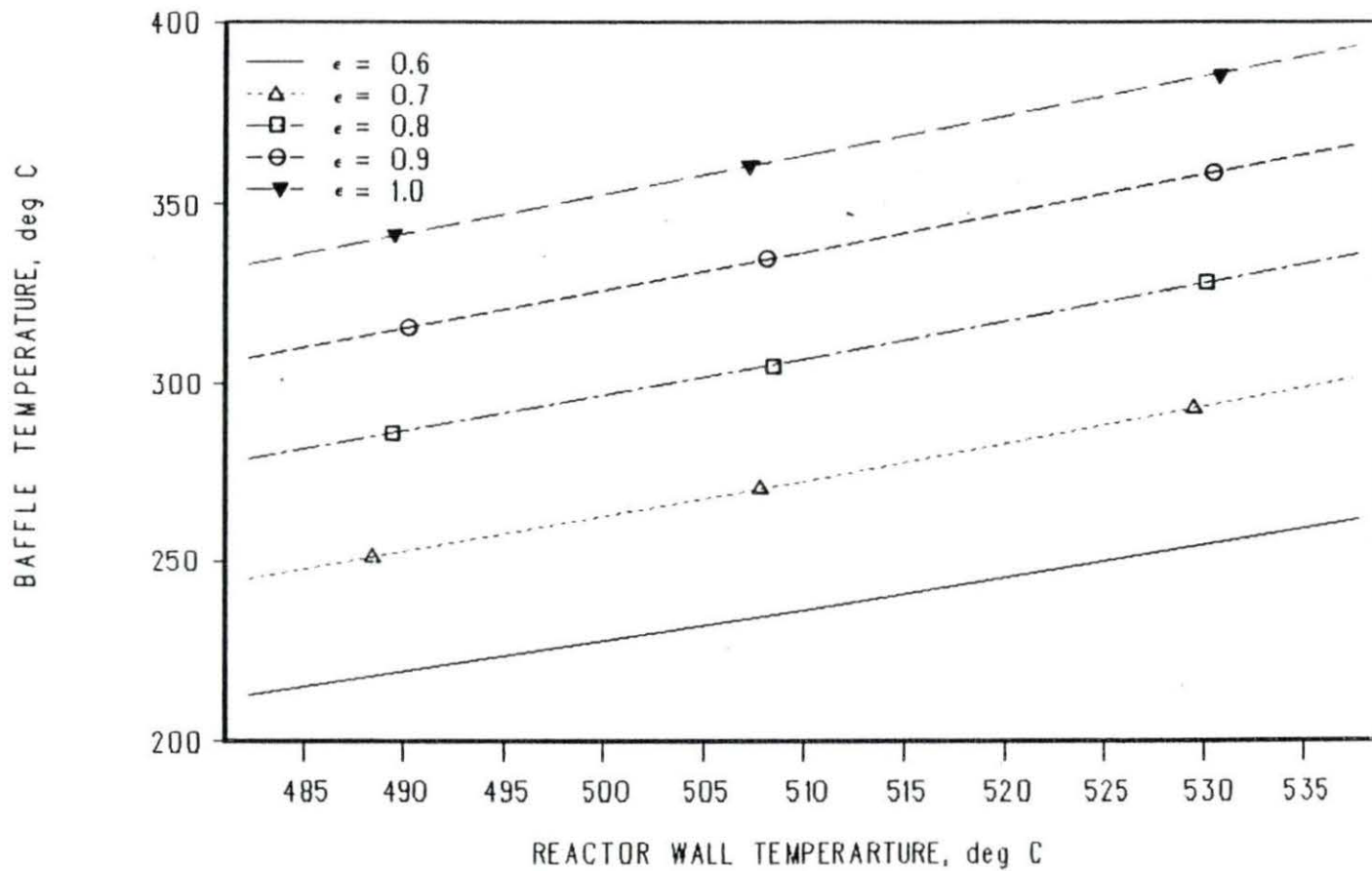


FIGURE 10. Baffle Temperature versus Wall Temperature for different values of ϵ , with $D = 1.5$ ft, $\Omega = 0.5$ and $T_{s_1} = 37.78^\circ$ C

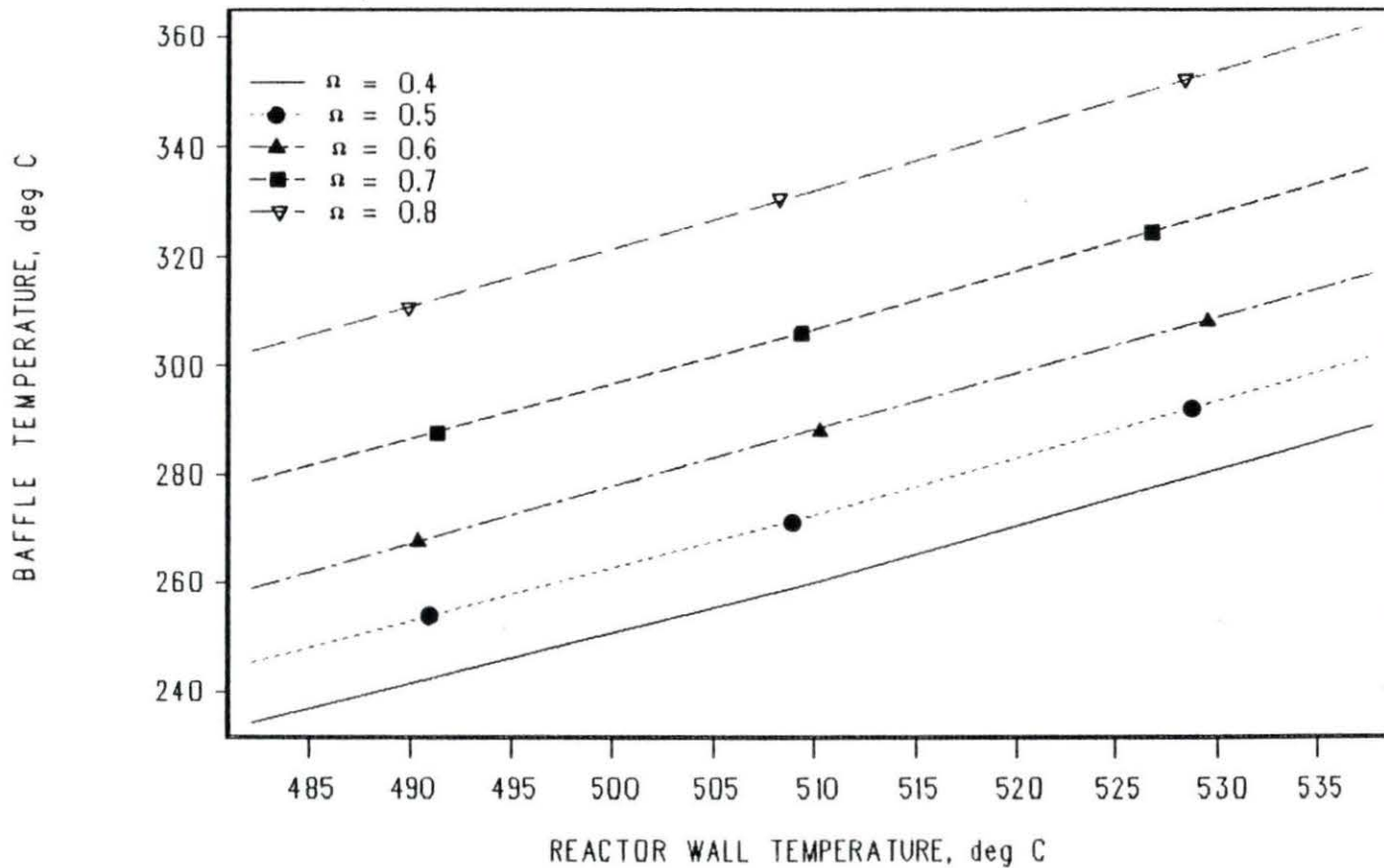


FIGURE 11. Baffle Temperature versus Wall Temperature for different values of Ω , with $D = 1.5$ ft, $\epsilon = 0.7$ and $T_{c,i} = 37.78^\circ$ C

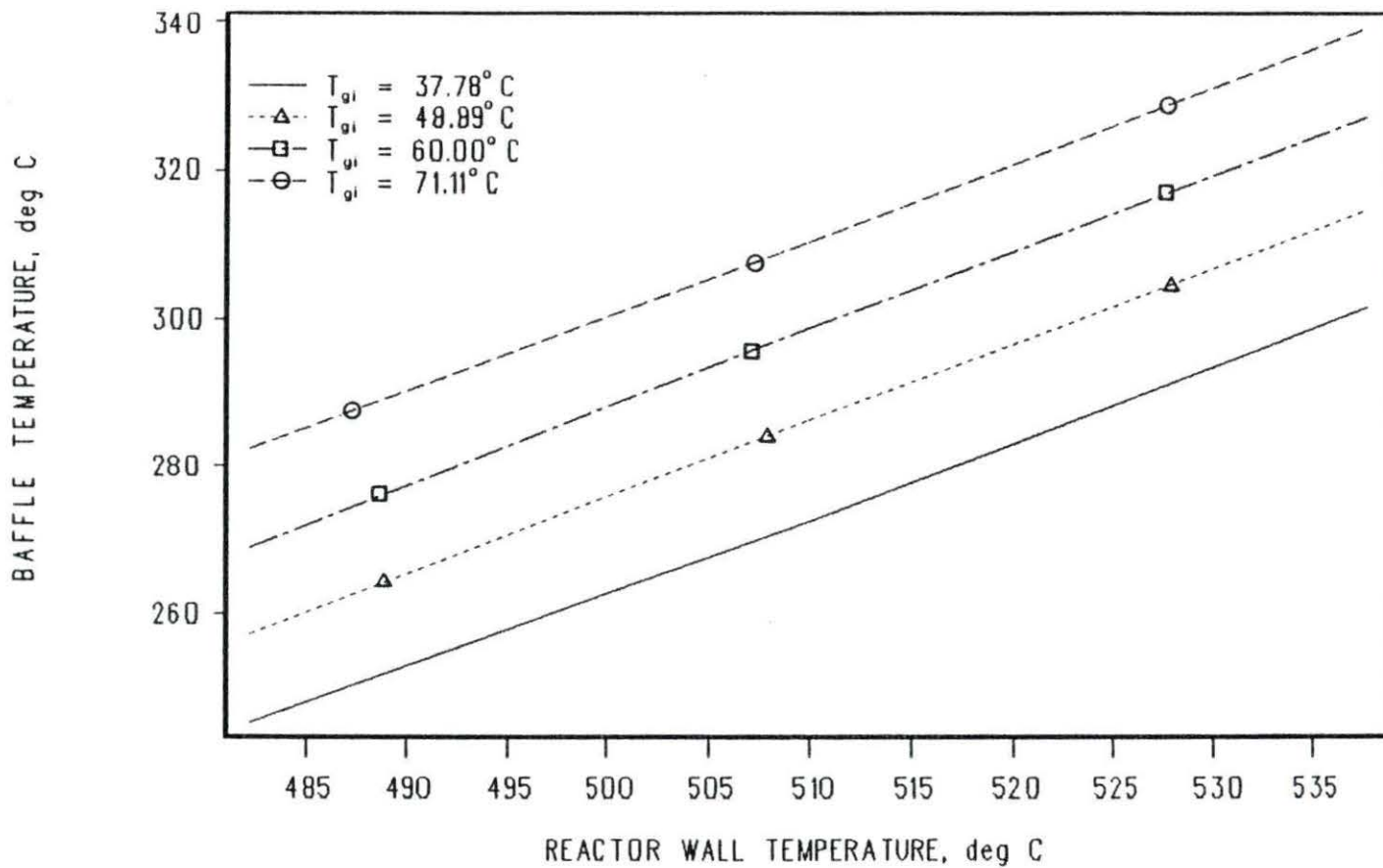


FIGURE 12. Baffle Temperature versus Wall Temperature for different values of T_{gi} , with $D = 1.5$ ft, $\epsilon = 0.7$ and $\Omega = 0.5$.

the values of T_w , higher will be the heat rejected to the gas. With increase in D , T_{g_o} decreases. As D increases, the mass flow rate of the gas increases. Thus, there is more fluid carrying the heat away which causes the average temperature as well as T_{g_o} to decrease.

The effect of ϵ on the outlet gas temperature is shown in Fig. 14. For higher values of ϵ , there is more radiation from the reactor walls to the baffle. Thus, there is more heat transferred to the gas from the baffle which causes T_{g_o} to be higher.

As seen in the Fig. 15, T_{g_o} increases as the value of Ω increases. As mentioned in the Section 4.1, $Q_{t_o t}$ decreases as Ω increases. The mass flow rate also decreases as Ω increases. However, the ratio of $Q_{t_o t}$ to the mass flow rate increases. This quantity is the difference between the outlet and inlet temperature for the channel. Thus, for the same T_{g_i} , T_{g_o} increases, although the increase is very small.

The effect of T_{g_i} on the outlet gas temperature for the inner channel as a function of T_w is shown in Fig. 16. As inlet temperature increases T_{g_o} increases since the gas is still getting heat from the walls and the baffle, though at a lesser rate.

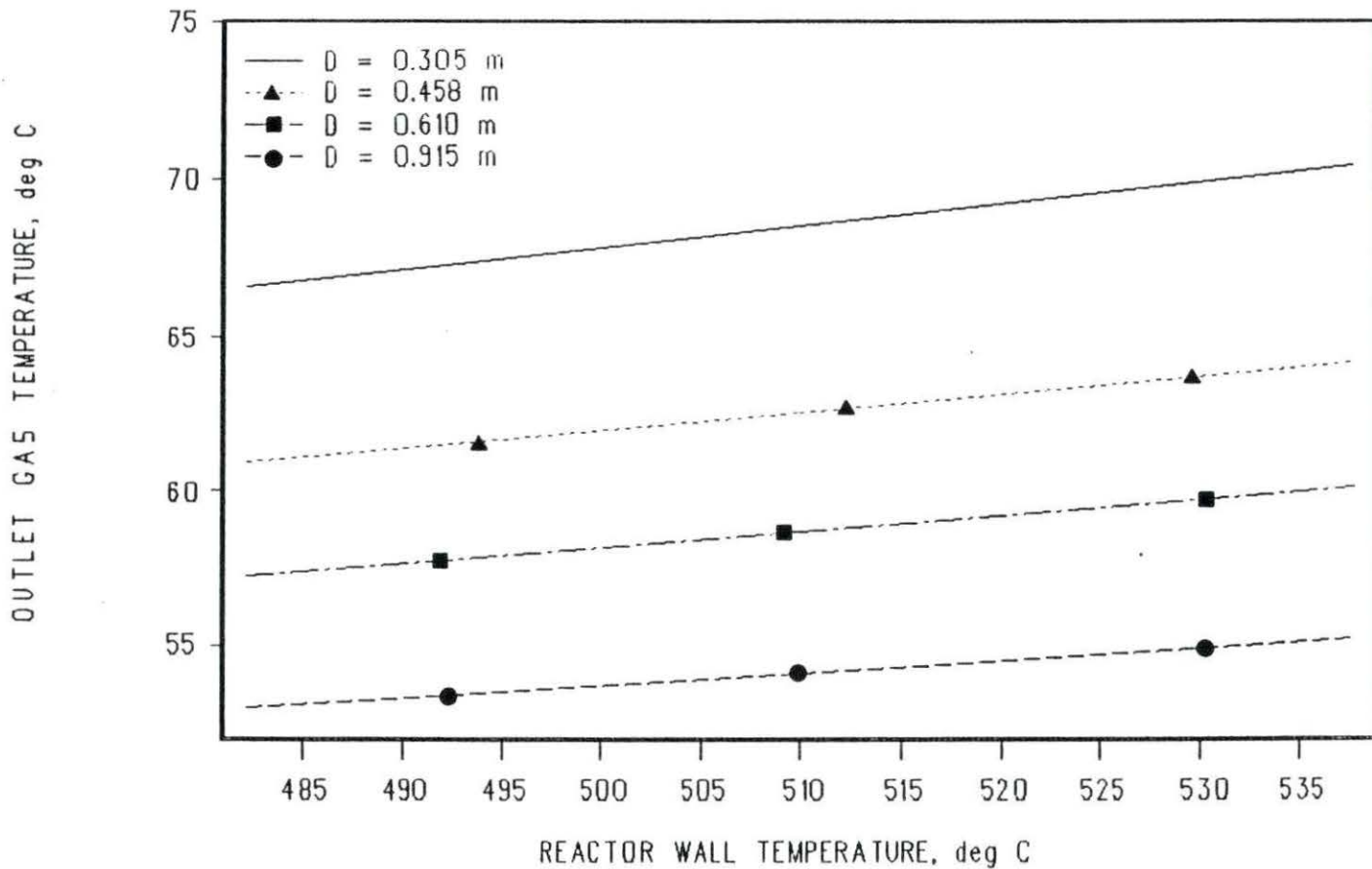


FIGURE 13. Channel Outlet Gas Temperature versus Wall Temperature for different values of D , with $\epsilon = 0.7$, $\Omega = 0.5$ and $T_{a1} = 37.78^\circ \text{C}$

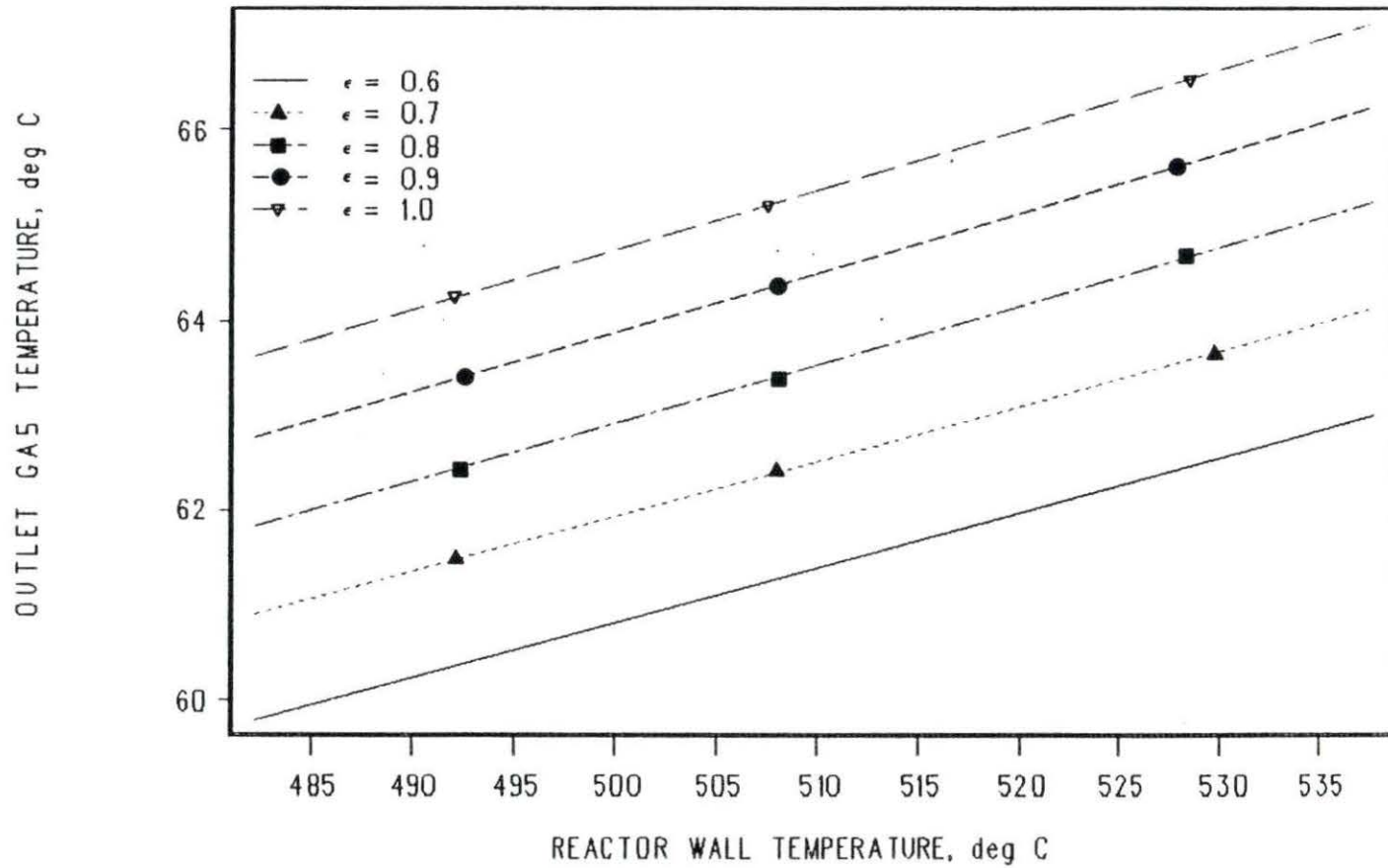


FIGURE 14. Channel Outlet Gas Temperature versus Wall Temperature for different values of ϵ , with $D = 1.5$ ft, $\Omega = 0.5$ and $T_{s,i} = 37.78^\circ$ C

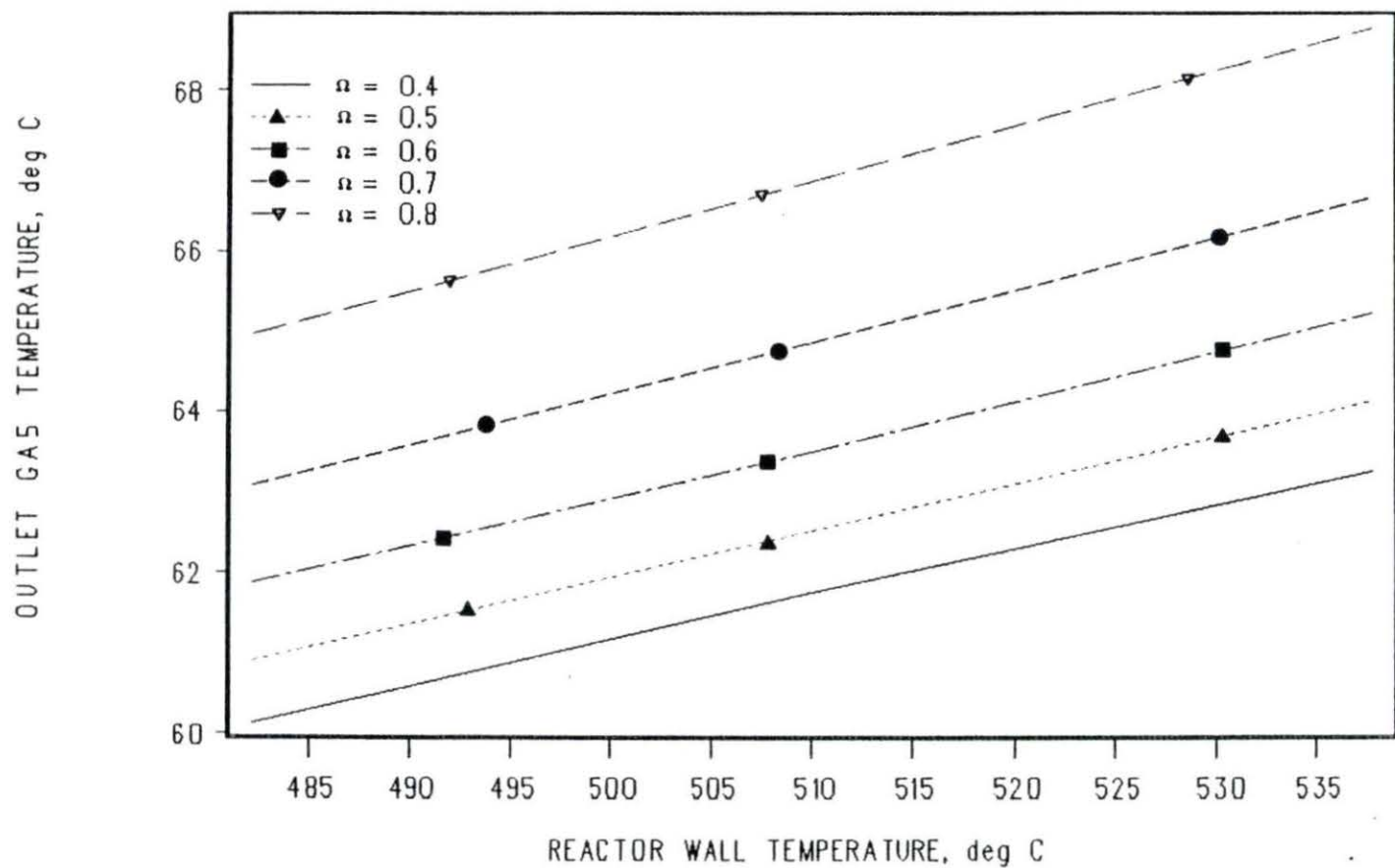


FIGURE 15. Channel Outlet Gas Temperature versus Wall Temperature for different values of Ω , with $D = 1.5$ ft, $\epsilon = 0.7$ and $T_{o,i} = 37.78^\circ$ C

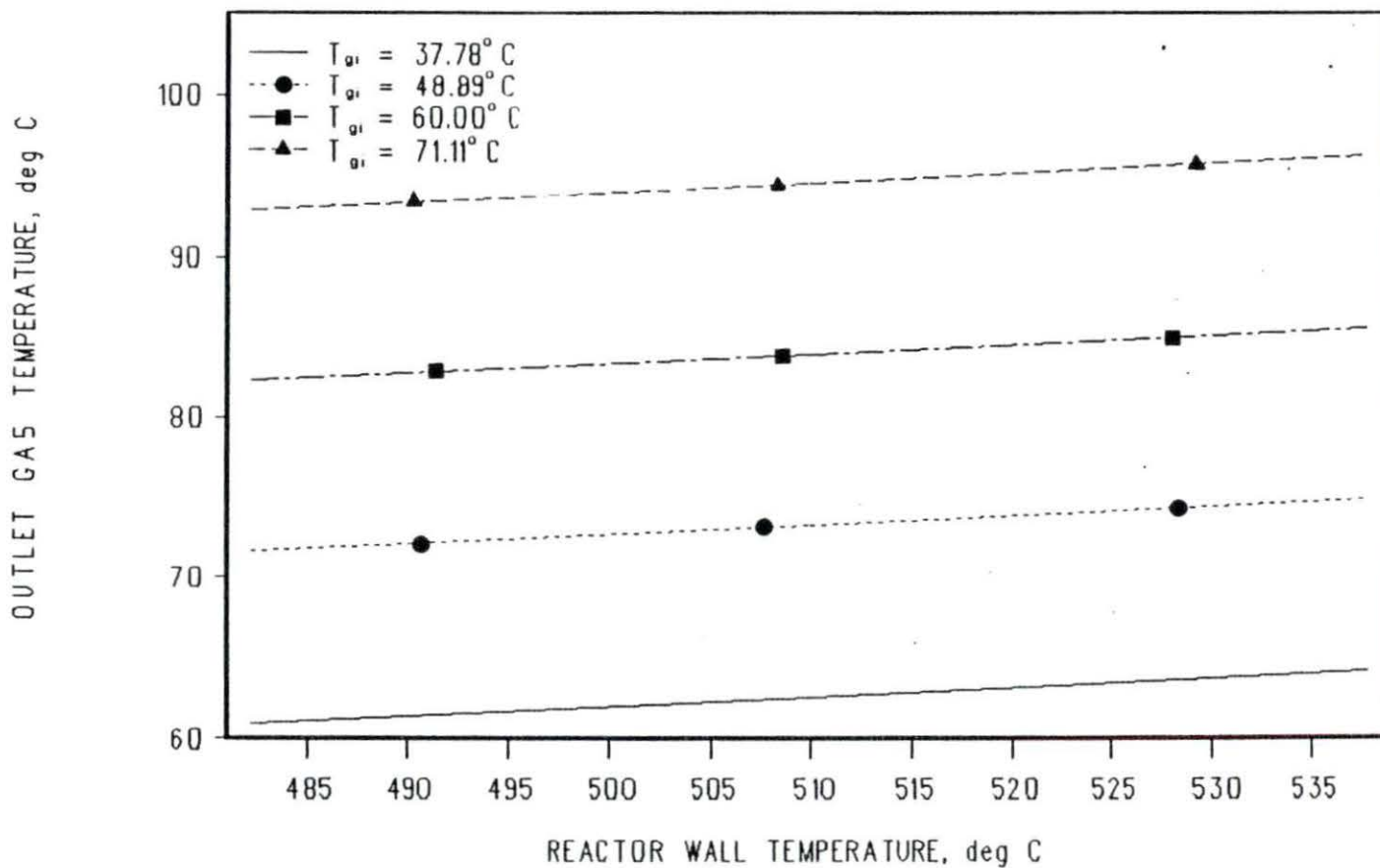


FIGURE 16. Channel Outlet Gas Temperature versus Wall Temperature for different values of T_{g_i} , with $D = 1.5$ ft, $\epsilon = 0.7$ and $\Omega = 0.5$

4.2 Transient Behavior of the System

The transient behavior of the T_w was numerically calculated by solving equation (3.38), and by putting in different functional forms of the heat loss term for the different values of important parameters considered in Section 4.1. For all the cases studied, the relation between $Q_{t.o.t}$ and T_w is linear. Hence $f(T_w)$ in equation (3.38) has a straight line form $aT_w + b$, where the slope a and the intercept b can be easily found using the results in Section 4.1. The results of the program include values of T_w at various times after shutdown. The interval for calculating and printing the values of T_w was taken to be 100 seconds. The runs were made for 5 hours after shutdown. The results of time-dependent values of the T_w have been used to calculate the time-dependent values of T_b and $T_{g.o.}$. From the results in the previous section, equations have been obtained for T_b as a function of T_w and $T_{g.o.}$ as a function of T_w for different values of ϵ , Ω and D . Using the relationship thus obtained, values of T_b and $T_{g.o.}$ have been calculated as a function of time by using the time-dependent values of T_w for given input conditions. The limiting case is where there is no cooling of the reactor vessel by the gas. This case was studied by making the heat loss term in the differential equation (3.38) as 0. The

expectation would be that the T_w will increase with time since there is some heat being generated inside the reactor in the form of decay heat, but there is no heat loss from the system. This is a hypothetical case, but is of interest nevertheless. The transient behavior of the T_w depends on $Q_{t \circ t}$ for the set of variables chosen.

4.2.1 Reactor wall temperature as a function of time

The transient behavior of T_w is directly related to $Q_{t \circ t}$ for given values of important input variables. For the limiting case of no cooling, T_w increases continuously with time. When the cooling term is introduced in equation (3.38), T_w increases, but very slowly compared to when it is not cooled. For the cooling cases studied here, T_w slowly increases and becomes steady or starts decreasing slowly within the first 5 hours after shutdown. Fig. 17 shows T_w as a function of time for different values of D . There is a very predominant effect of D on T_w since D also has a significant effect on $Q_{t \circ t}$ as shown in Fig. 5. $Q_{t \circ t}$ increases as D increases. Thus, there is more cooling of the reactor walls and the maximum T_w becomes lower, and is attained earlier too. For a value of D of 3.0 ft, after a little more than 2 hours, T_w decreases to values below what its value was at the time of shutdown after a little more than 2 hours.

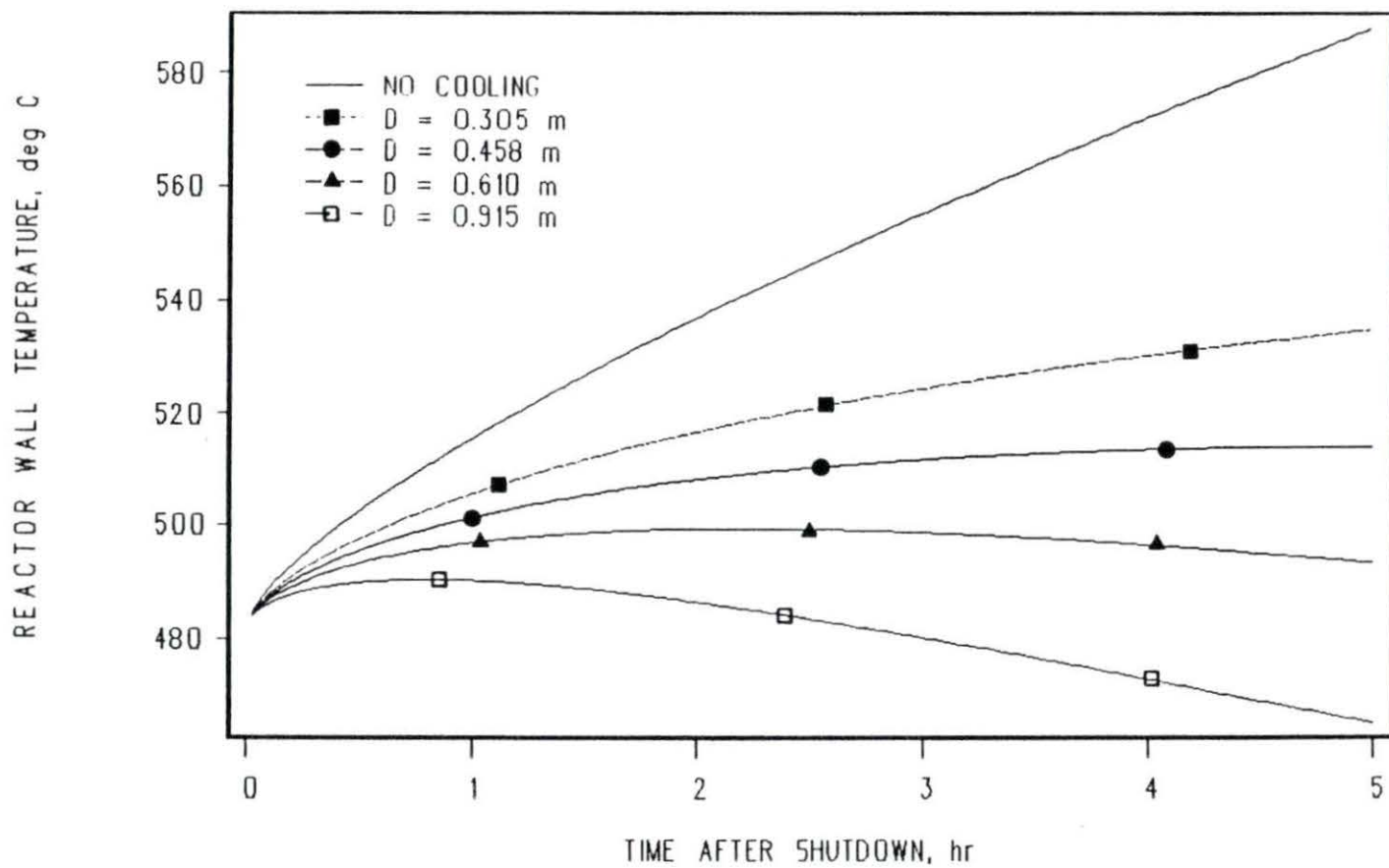


FIGURE 17. Wall Temperature versus Time for different values of D , with $\epsilon = 0.7$, $\Omega = 0.5$ and $T_{s,i} = 37.78^\circ \text{C}$

The effect of ϵ on the transient behavior of T_w is shown in Fig. 18. As ϵ increases, the heat lost by radiation increases, and therefore T_w decreases.

Fig. 19 shows plots of T_w versus time with the other independent variable as Ω . As Ω increases from 0.4 to 0.8, the maximum T_w becomes higher since $Q_{t \rightarrow t}$ decreases as shown in Fig. 7 in Section 4.1.

4.2.2 Baffle temperature and gas outlet temperature as a function of time

Both T_b and T_{g_o} behave essentially in the same manner as T_w . Fig. 20, Fig. 21, and Fig. 22 show the transient behavior of T_b as a function of D , ϵ and Ω , respectively. Similar plots for T_{g_o} are given in the same order in Fig. 23, Fig. 24 and Fig. 25.

It can be seen readily from Figures 20 through 25 that both the T_b and T_{g_o} exhibit a transient behavior similar to that of the T_w . It should be noted here that the initial condition stated in Chapter 3 implies that T_w , is the same (482.22°C or 900°F) at the time of shutdown for all the cases studied. However, the values of T_b and T_{g_o} are different for different values of D , ϵ and Ω , since they are calculated for the given conditions using the wall temperature. One of the similarities in the plots for all

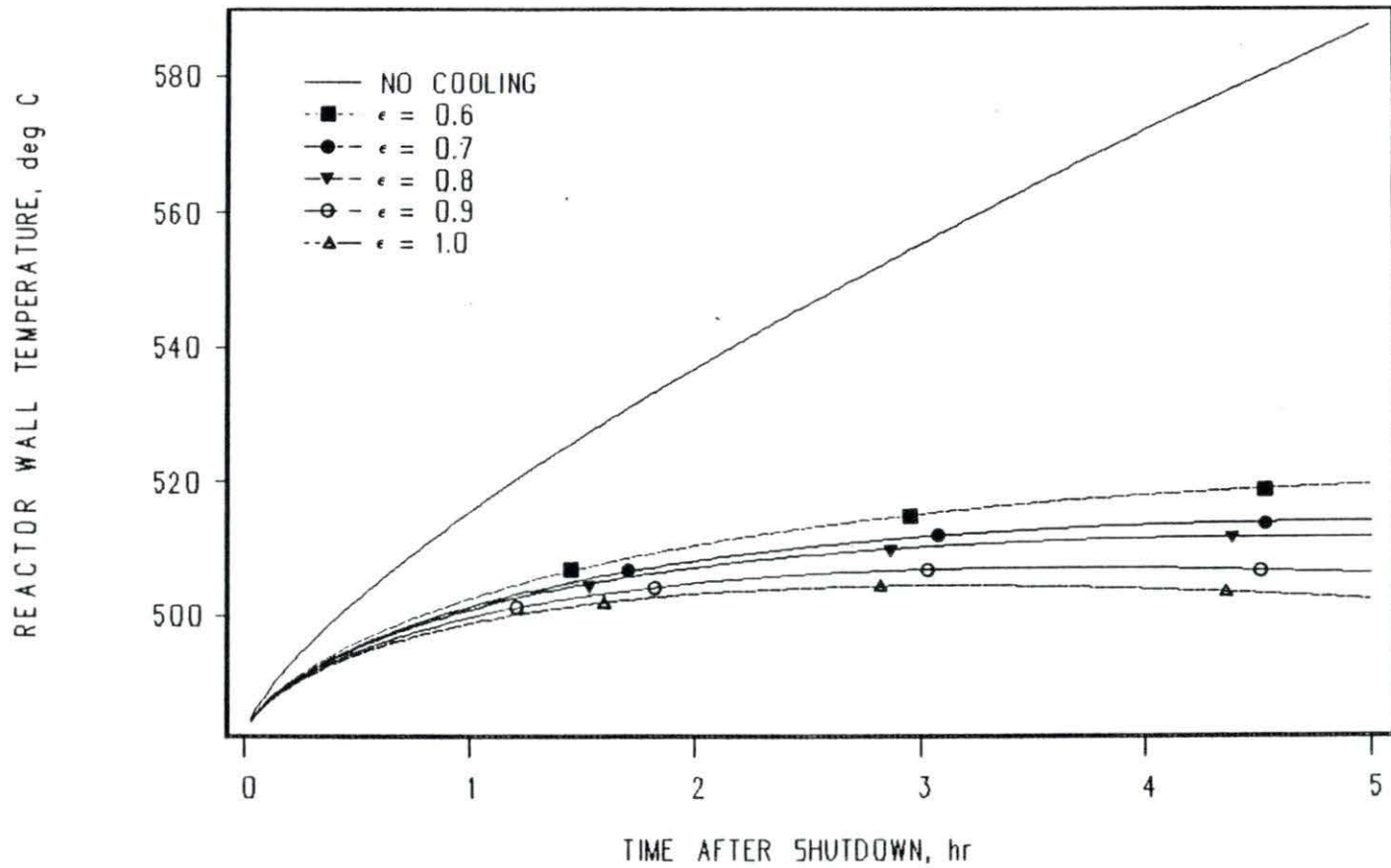


FIGURE 18. Wall Temperature versus Time for different values of ϵ , with $D = 1.5$ ft, $\Omega = 0.5$ and $T_{s,i} = 37.78^\circ \text{C}$

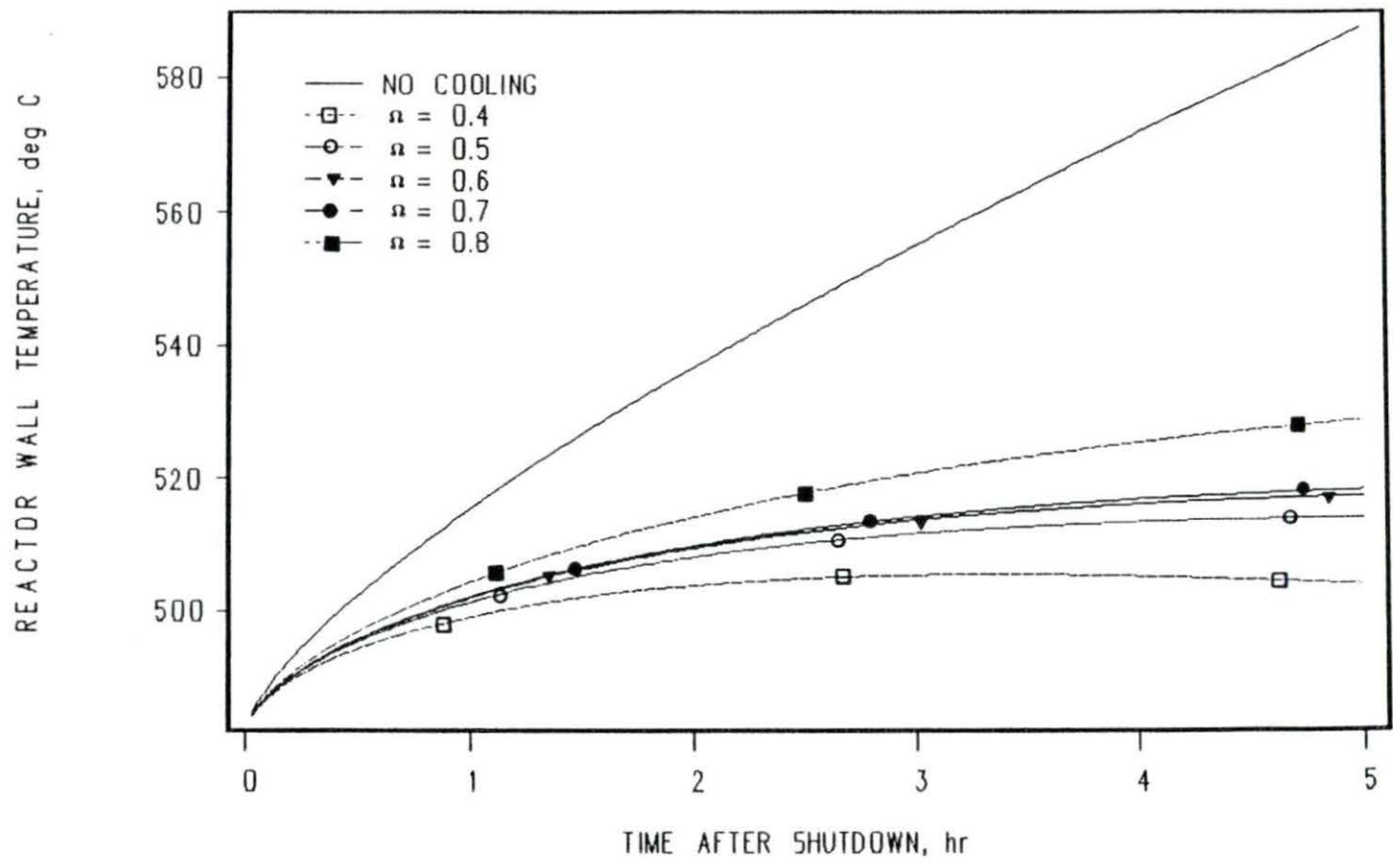


FIGURE 19. Wall Temperature versus Time for different values of Ω , with $D = 1.5$ ft, $\epsilon = 0.7$ and $T_{s,i} = 37.78^\circ \text{C}$

the three variables is that all of them either become steady or start decreasing very slightly over the period of time for which the plots are made. All of them decrease with an increase in D , decrease with an increase in ϵ , and increase with an increase in Ω . The reasons for such a behavior of T_w are mentioned in Section 4.2.1.

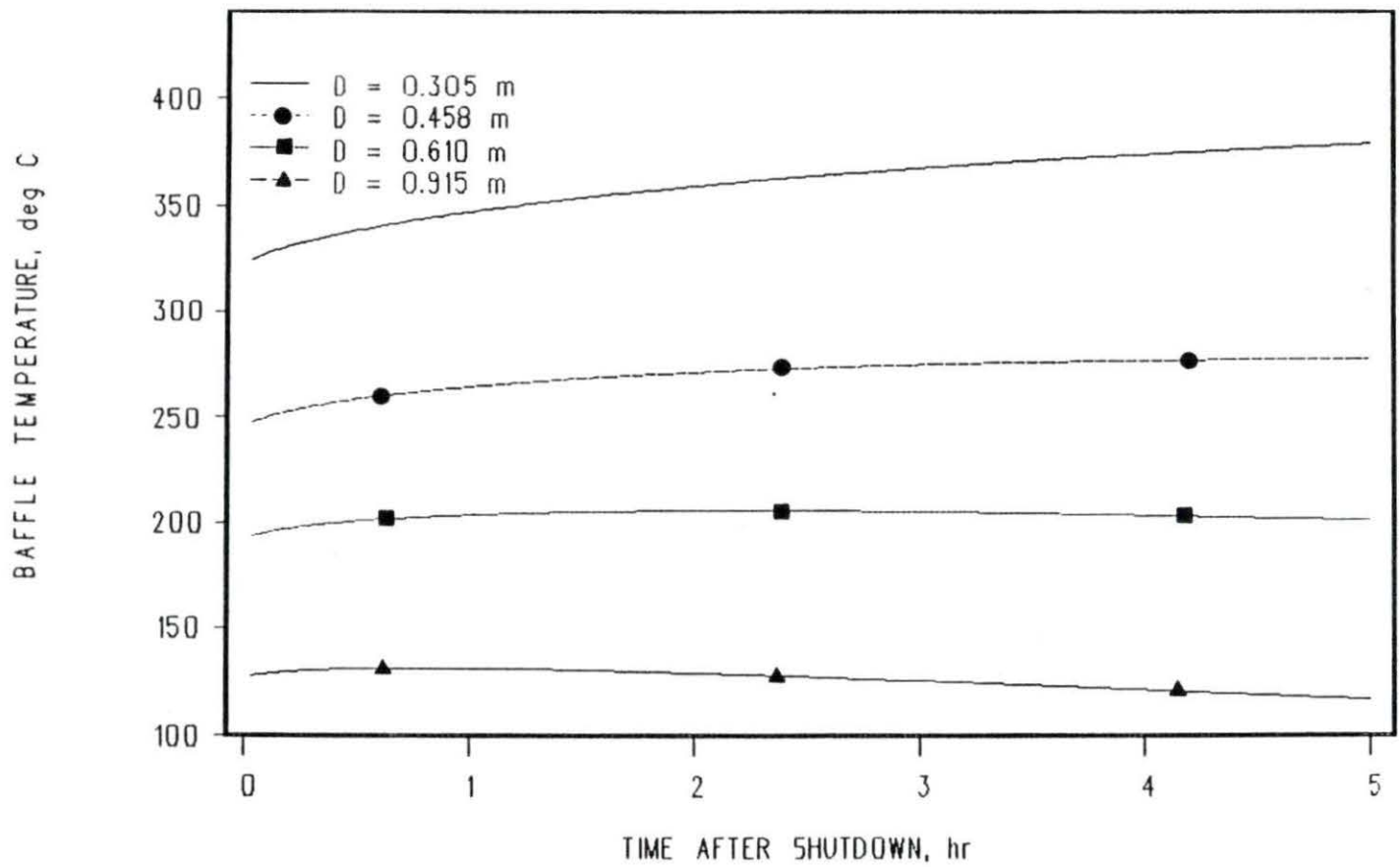


FIGURE 20. Baffle Temperature versus Time for different values of D , with $\epsilon = 0.7$, $\Omega = 0.5$ and $T_{s,i} = 37.78^\circ \text{C}$

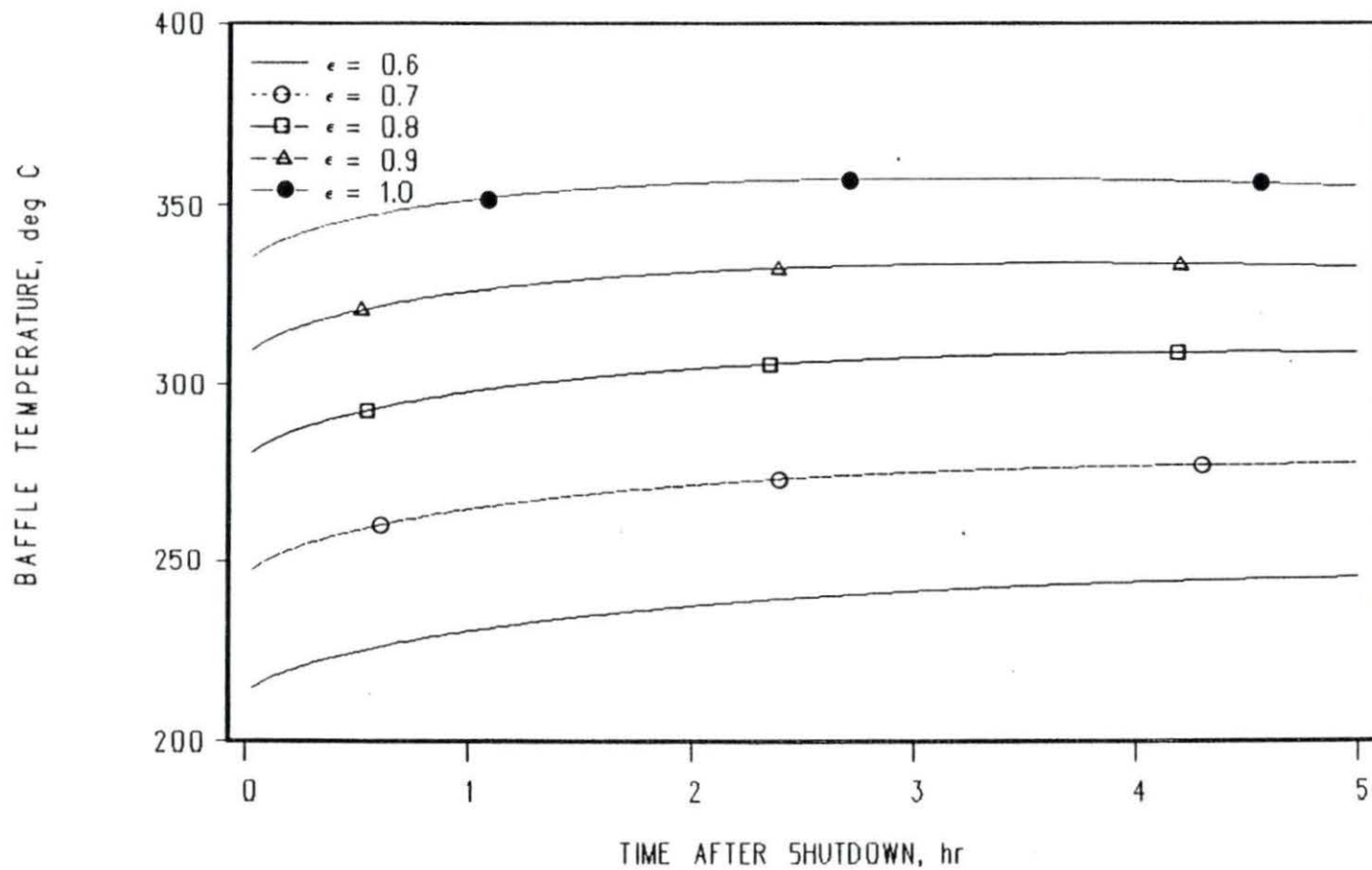


FIGURE 21. Baffle Temperature versus Time for different values of ϵ , with $D = 1.5$ ft, $\Omega = 0.5$ and $T_{s,i} = 37.78^\circ \text{C}$

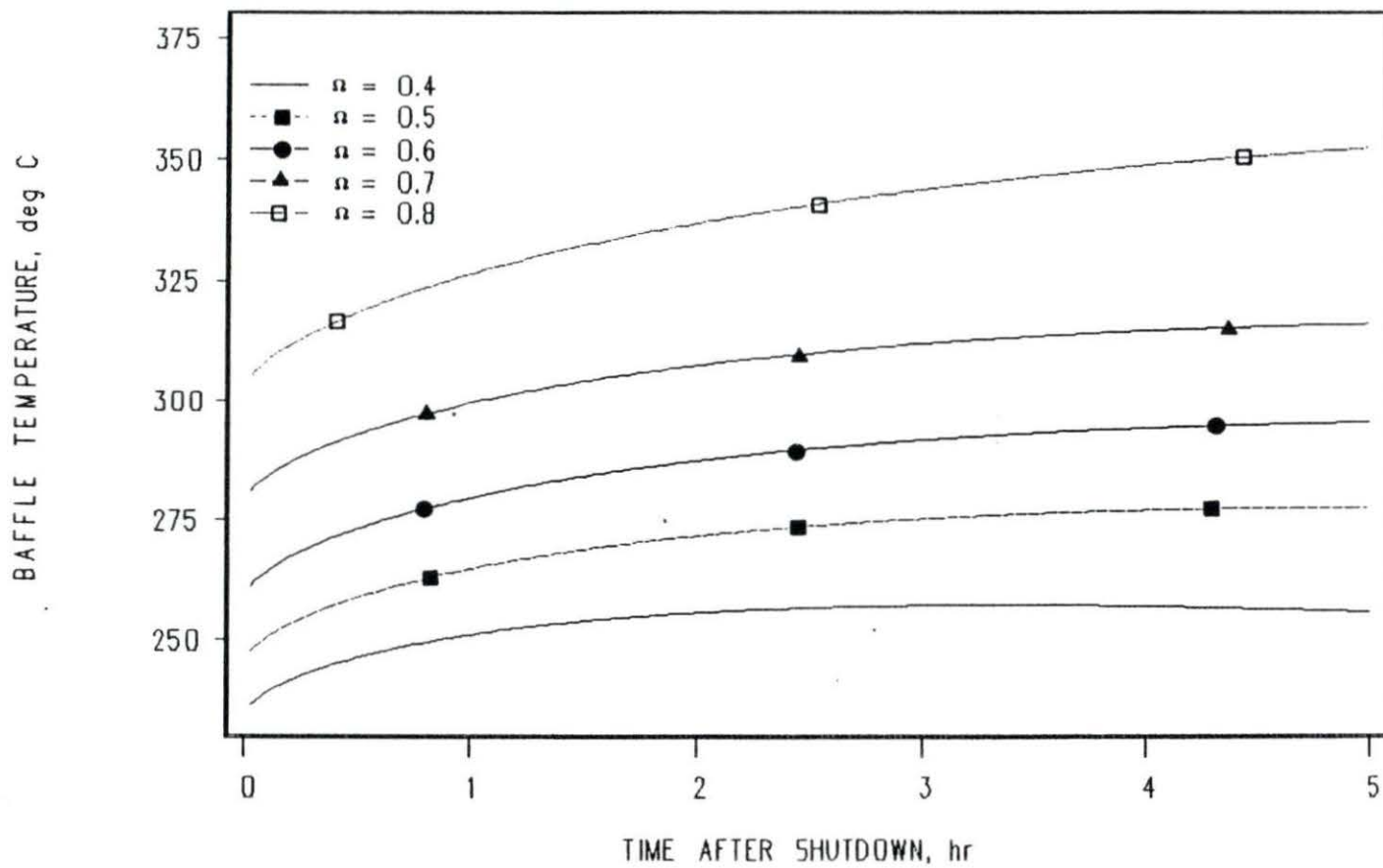


FIGURE 22. Baffle Temperature versus Time for different values of Ω , with $D = 1.5$ ft, $e = 0.7$ and $T_{u,i} = 37.78^\circ \text{C}$

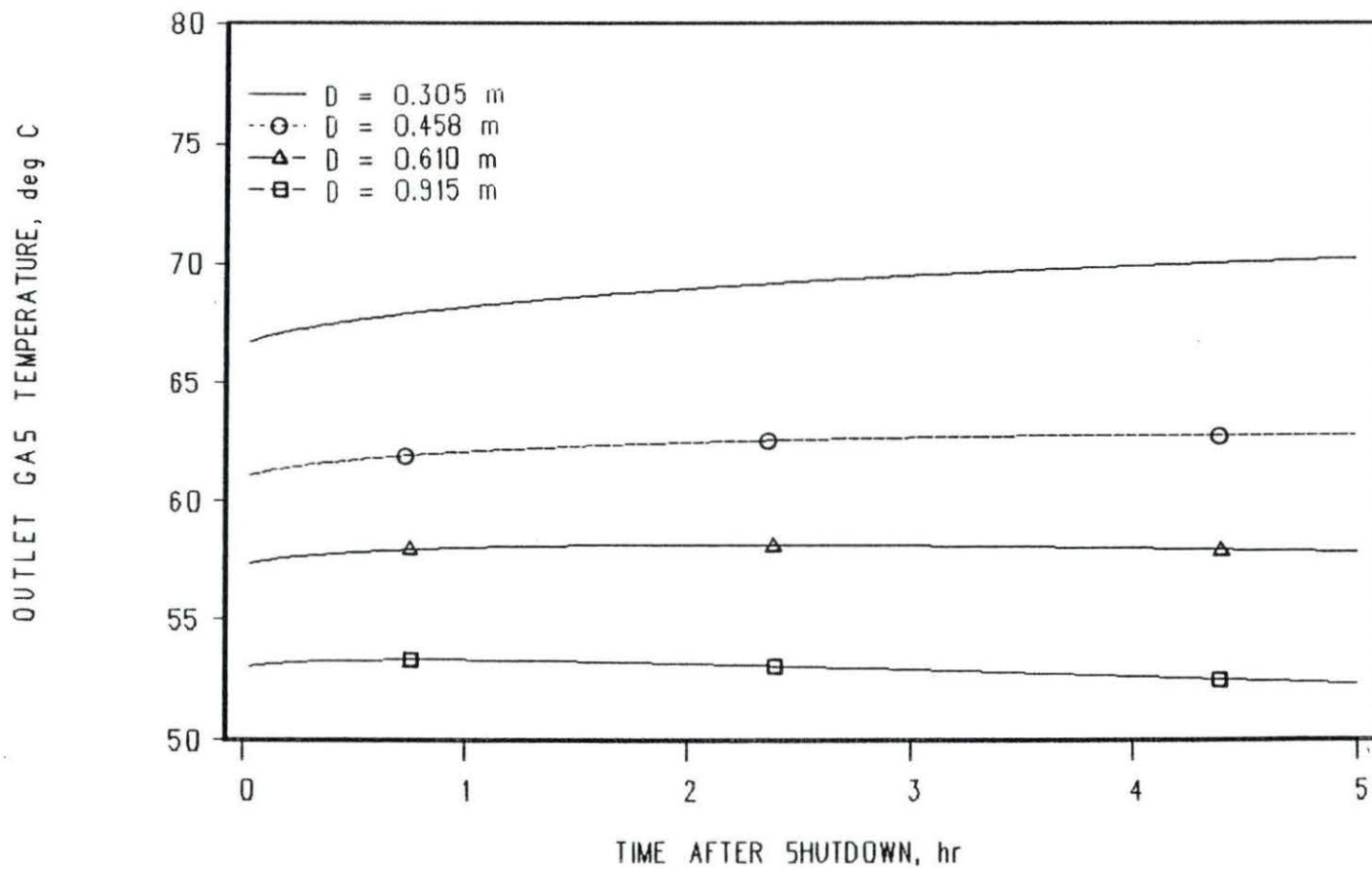


FIGURE 23. Gas Outlet Temperature versus Time for different values of D , with $e = 0.7$, $\Omega = 0.5$ and $T_{a,i} = 37.78^\circ \text{C}$

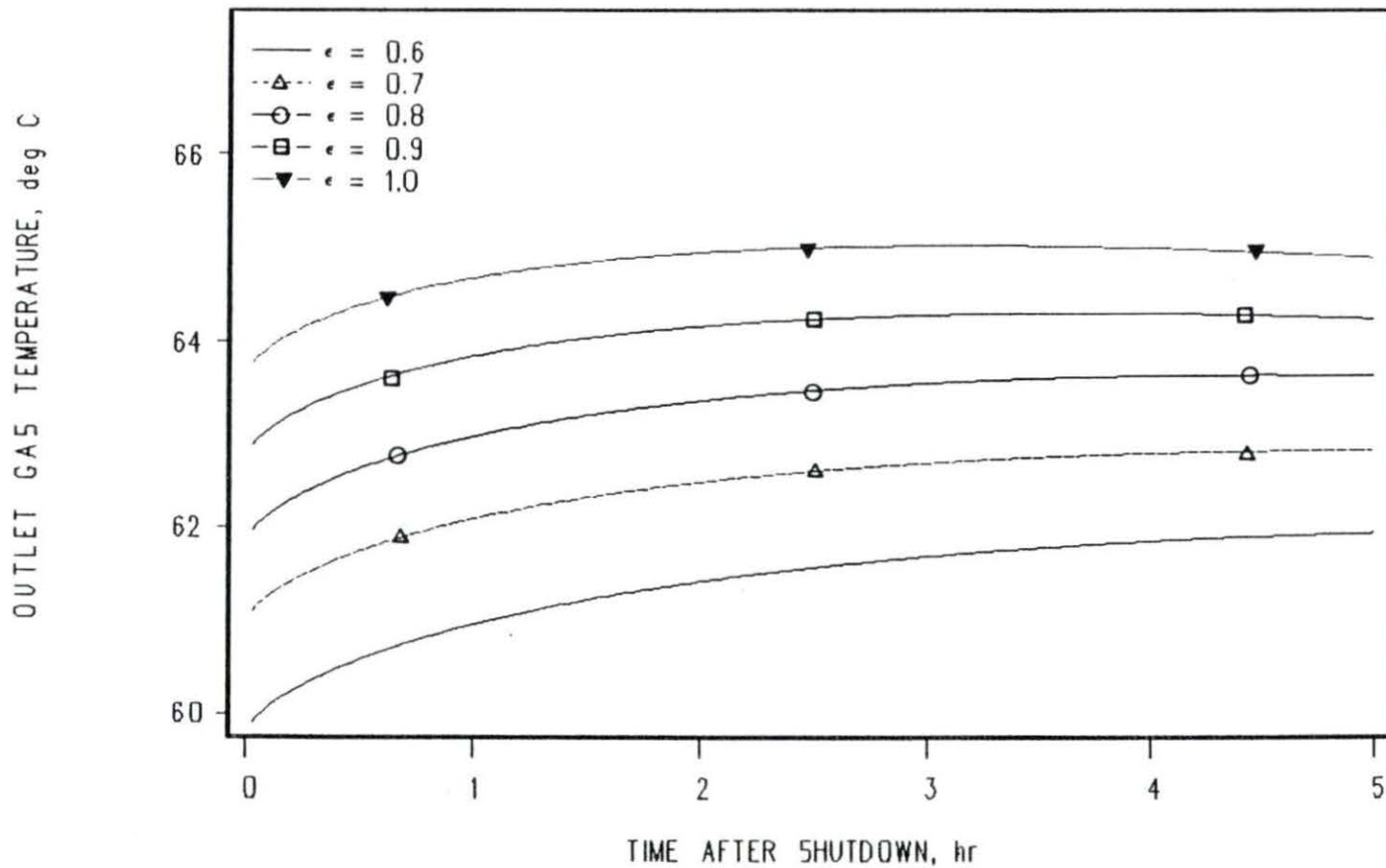


FIGURE 24. Gas Outlet Temperature versus Time for different values of ϵ , with $D = 1.5$ ft, $\Omega = 0.5$ and $T_{s,i} = 37.78^\circ$ C

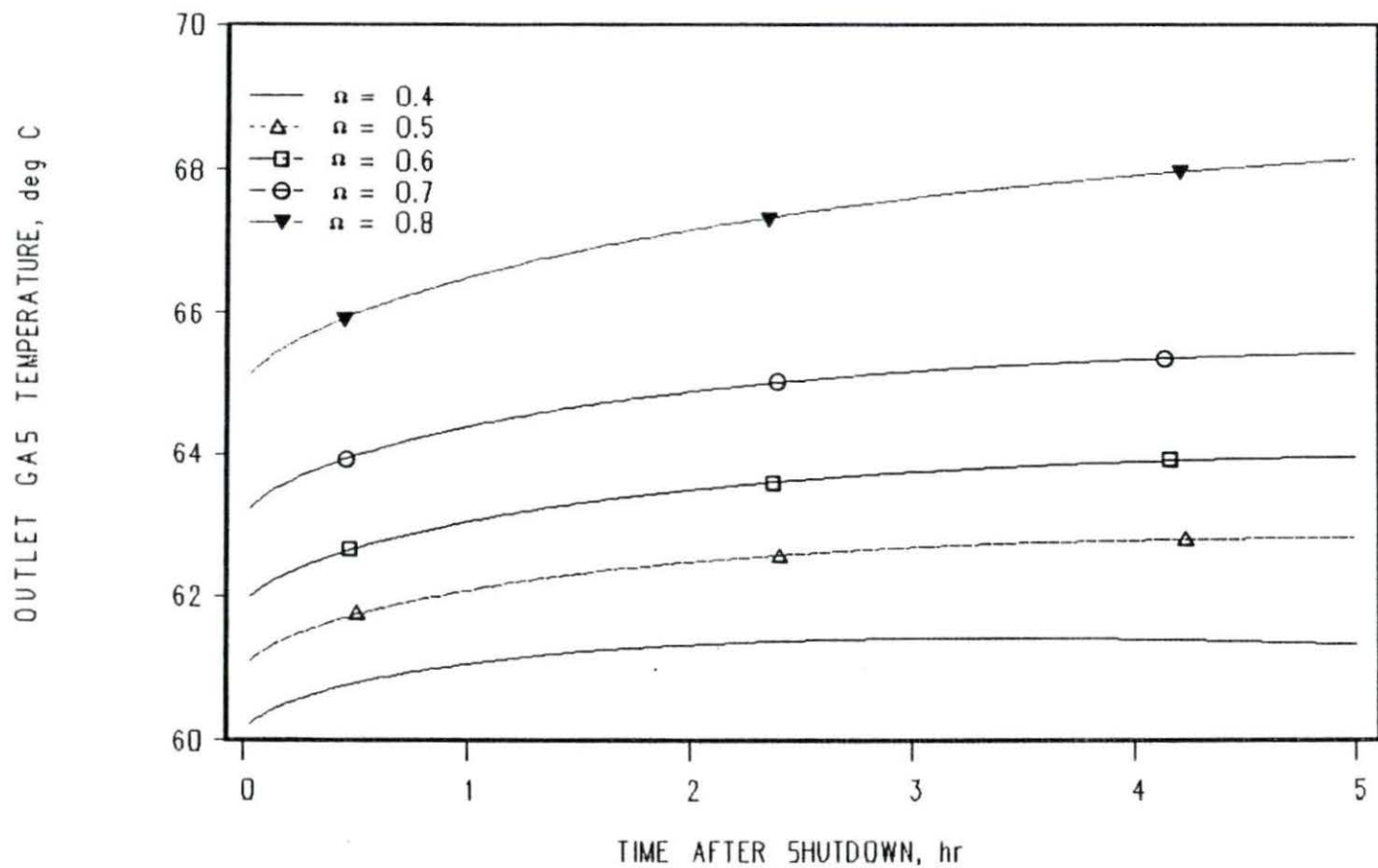


FIGURE 25. Gas Outlet Temperature versus Time for different values of Ω , with $D = 1.5$ ft, $\epsilon = 0.7$ and $T_{a,i} = 37.78^\circ \text{C}$

5. CRITICAL EVALUATION, SUMMARY AND CONCLUSIONS

The critical evaluation of the present study is made first in this Chapter. This includes comments on the assumptions made in the present study that were stated in Chapter 3, the limitations of using these assumptions and how they would introduce errors in the analysis and solution of the problem. A summary of the present study and conclusions are stated in the end.

5.1 Critical Evaluation of Present Study

The assumptions stated in Chapter 3 indicate that in the present study, a very complex physical situation has been modeled as a simple system. The method of solution that has been employed is numerical and is not a detailed analytical study of the natural circulation cooling of a reactor vessel having a rectangular geometry where the flow channel is formed by two walls at different temperatures.

There are some assumptions in this study that might cause errors in the calculations and the results thus obtained. As already mentioned in Chapter 3, the approximation of a fully developed turbulent flow with a velocity profile similar to fully developed, turbulent, forced convection flow makes the problem simple to model and solve. Assuming that the flow is fully developed, turbulent

flow also introduces error in this analysis in the use of the correlations for the friction factor and frictional pressure drop in the inner channel as well as the correlation for Nusselt number. It is suspected that the flow may have a considerable entry length and as such, the entry length may play important part as far as the heat transfer is concerned. It has also been assumed that the baffle is at a uniform temperature. This would contribute to the error in the calculations since the baffle is a long thin plate insulated on one side, and is expected to have a non-uniform temperature distribution in the direction of flow. The transient heat transfer problem of the cooling of the reactor walls has been solved as a series of steady state cases. However, the heat loss term would have to account for the time dependence of the gas temperature and the baffle temperature. Replacing the heat loss term as a function of the wall temperature would introduce an error in the transient analysis. The empirical value of Ω is an important variable and a more realistic estimate of the true value of Ω would give more realistic results. However, the present study considered a range of values of Ω and hence can be used to predict the effect of Ω on the results. The decoupling of radiation and convection heat transfer is a simplification of the situation but would introduce errors

in the calculation. However, to couple radiative and convective heat transfer would render the problem very complex and difficult to model and solve.

5.2 Summary and Conclusions

The cooling after shutdown of the sodium cooled trench reactor with an operating power of 800 MW(th) by natural circulation of gas was studied by a numerical method. A baffle put at an appropriate distance from the reactor walls forms channels between the reactor walls and the biological shield. The reactor walls lose heat by convection to the gas and by radiation to the baffle. The heat entering into the baffle by radiation is rejected to the gas by convection. An iterative procedure was employed to calculate the heat removal rate and other important parameters such as the baffle temperature and the outlet temperature of the gas for the channel in which it is heated. The channel was divided into a number of nodes of equal height. For each node, heat rejected by convection by the reactor walls and the baffle was equated to the increase in enthalpy of the gas. The flow was assumed to be a fully developed, turbulent, forced convection flow. The velocity of the gas was obtained by equating buoyancy with the total pressure drop in the circuit. The friction factor was calculated using Blasius

equation [10] for smooth pipes. Sieder-Tate correlation was used to calculate the heat transfer coefficient for a node.

The heat removal rate was found as a function of reactor wall temperature. This functional form was used as the heat loss term in the transient heat transfer equation. This equation was obtained by equating the accumulation of heat in the sodium pool to the difference between heat generation in the pool and the heat loss from the reactor. The pool temperature and the reactor wall temperature were assumed to be equal. The heat generation term was the decay heat term for a LMFBR with large fuel burn-ups [8]. The transient equation which is a nonlinear ordinary differential equation, was solved by using the subroutine LSODA from the library ODEPACK on NAS AS/9160 computing system at Iowa State University.

From the results obtained, the following conclusions can be made:

1. For values of ϵ equal to 0.7, Ω equal to 0.5, and D equal to 1.5 ft, which are easily achievable, the heat removal rate was found to be about 6.5 MW which is adequate to cool the trench reactor.
2. D is the parameter that significantly affects the results. With an increase in D from 0.3048 m (1 ft) to 0.6096 m (2 ft), the heat removal rate

increased from 4.75 MW to 9.00 MW for reactor wall temperature equal to 537.78° C (1000.0° F). ϵ and Ω also affect the results though not as much as D.

6. SUGGESTIONS FOR FUTURE WORK

As seen from the evaluation of this study, there are many limitations to the analysis described here. However, it is a first attempt at studying this phenomenon. Future work is needed to better model, analyze and solve this problem. The ultimate goal of the present study is to maximize the heat removal rate and thus in turn to keep the highest wall temperature after shutdown at a minimum possible. This needs to be kept in mind when doing further work in this area, numerical, analytical or experimental.

- The present work is a primary study of this very complex physical situation. Future work should be directed towards improving the methodology based on the physical situation found by performing an analytical study of this phenomenon. Different areas in which analysis can be performed are listed below.
 1. Using the conservation of mass, transfer of momentum and energy equations, the velocity and temperature distribution in the channel needs to be determined.
 2. One needs to calculate the thermal entry length and the hydraulic entry length (i.e., the length over which the velocity

profile is not yet fully developed) and use correlations corresponding to the findings to make predictions about the heat transfer.

3. Assuming a developing flow, by numerical methods one needs to find parameters like Reynolds number that were basis for the assumptions about the flow conditions that were made in this study. Using the results, the methodology should be modified accordingly.
4. In going from the outer channel into the inner channel, the flow turns around the corner. Therefore, there will be a region of separated flow along the baffle. The length over which there is separated flow needs to be determined. Also, the thickness of the boundary layer of the separated flow needs to be determined. This information then needs to be incorporated in the analysis of the problem.
5. As mentioned in Chapter 3, a more detailed analysis needs to be performed to calculate

the true entrance-exit pressure loss for the flow conditions in the inner channel.

- Experimental work also needs to be performed to find the velocity and temperature distribution in the inner channel. The assumption about the flow conditions were forced by the lack of correlations for the system studied here. Thus, experimental data can be used to derive correlations for the frictional pressure drop and for the heat transfer coefficient or Nusselt number.
- As mentioned in Chapter 3, the decay heat generation term in the differential equation is a semi-empirical correlation for LMFBRs. A more exact evaluation should be done for the type of fuel used in the trench reactor using data from Chung [12] and the ANS standard [13].
- The present analysis has been performed assuming that there is no chimney at the top of the inner channel. An addition of chimney would help the heat transfer since it would cause the average density in the inner channel to be lower. This would increase the average velocity of the gas in the inner channel causing a higher heat transfer rate. However, a long chimney would be expensive and inconvenient.

- The effect of variation of baffle temperature in one or more dimensions on the heat transfer needs to be studied.
- The present study assumes that the inlet temperature is constant at all times, i.e., the gas rejects all the heat it picks up in the inner channel to the heat exchangers located in the ceiling of the containment building. For the case when these heat exchangers do not perform well, the gas won't be cooled adequately and as a result, the inlet temperature would increase with time. This phenomenon needs to be studied in order to know how the reactor wall temperature would change with time including the change in inlet temperature in the analysis. It is also important to know what the maximum reactor wall temperature will be for such a case.
- The surface characteristics of the reactor walls and the baffle are important as far as the results are concerned. The present study assumed that the reactor walls and the baffle both have surfaces similar to that for commercial pipes. Surface roughness would increase the frictional pressure drop and at the same time enhance turbulence.

Thus, the effect of different kinds of surfaces on the heat transfer needs to be studied. The results of such a study can be used to determine which type of surface is the best.

- The present analysis considered both reactor walls and the baffle to have flat surface. Some sort of turbulence promoters (e.g., spikes or thin fins) can be put on either the reactor walls, or the baffle plate or on both as shown in Fig. 26. Each of these would enhance the heat transfer compared to flat walls. However, a detailed study needs to be performed to find out the effect of each of these cases on the heat transfer and then use the configuration that provides the maximum heat removal.
- One of the minor modifications that can be introduced in the present analysis is the use of different emissivity values for the reactor walls and the baffle. This would change the equation (3.33) which is used to find a new value of the baffle temperature by equating the radiation from the reactor walls to the baffle with the convection from the baffle to the containment gas.

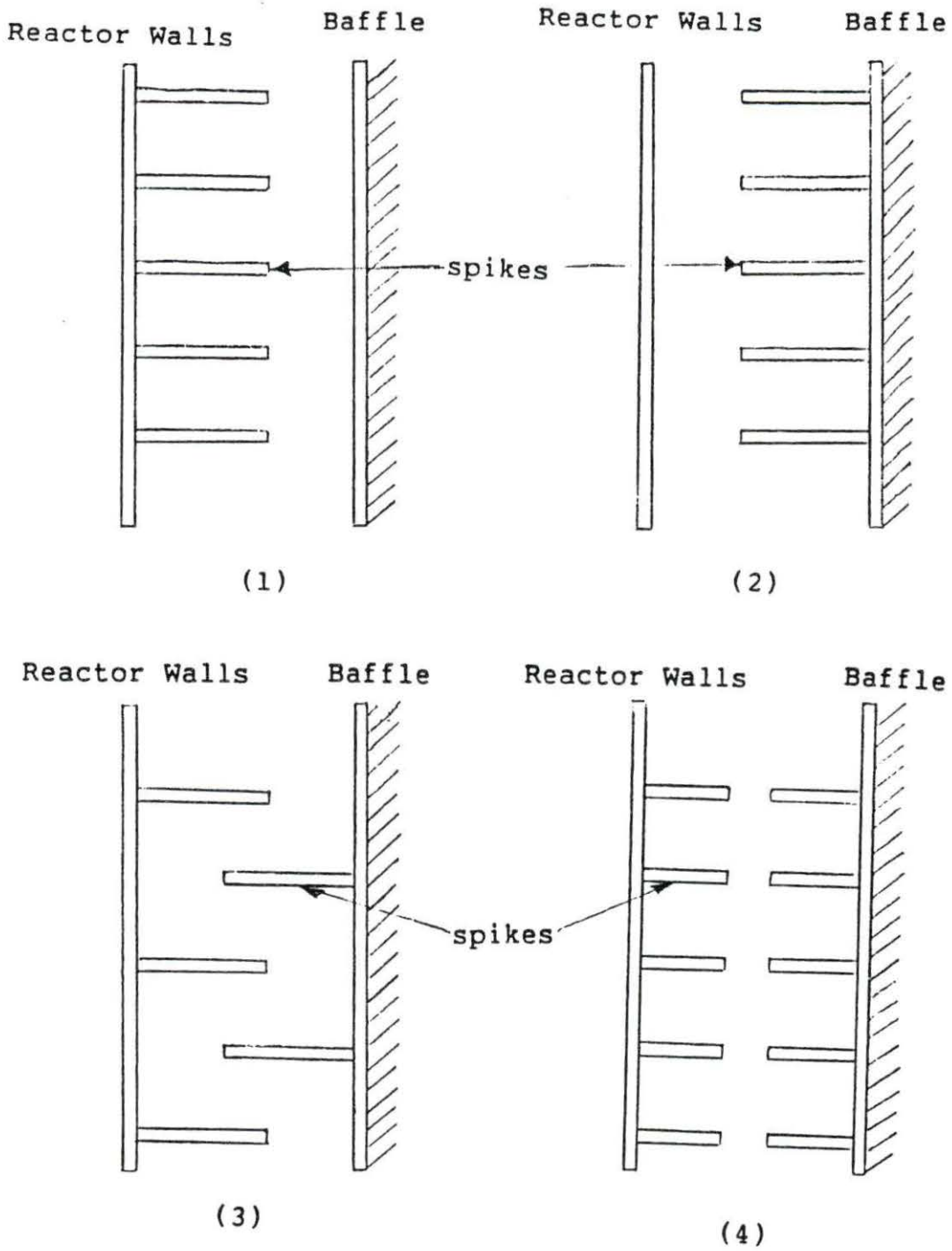


FIGURE 26. Possible Configurations for the Inner Channel

7. BIBLIOGRAPHY

1. T. C. Chawla et al. "Modeling of the Air-side Performance of the RVACS Shutdown Heat Removal System--Status of Experimental Program". ANL-PRISM-8, 1985.
2. B. I. Spinrad. "Unconventional Liquid Metal Cooled Fast Power Reactor Concepts". Proposal to U.S. Department of Energy, 1985.
3. R.D. Coffield et al. "Performance Characteristics of a Reactor Vessel Air-Cooling Concept for LMR Shutdown Heat Removal". Trans. ANS, 50, pp. 337-339, 1985.
4. J. R. Lamarsh. Introduction to Nuclear Engineering. 2nd edition. Addison-Wesley Publishing Co., Reading, Massachusetts, 1983.
5. A. M. Judd. Fast Breeder Reactors- An Engineering Introduction. Pergamon Press, Oxford, England, 1981.
6. M. Debry et al. "Decay Heat Removal in SUPER PHENIX and Related Design Basis Plant Conditions". In Decay Heat Removal and Natural Convection in fast Breeder Reactors, pp. 263-273. Edited by A. K. Agrawal and J. G. Guppy. Hemisphere Publishing Co., Washington, 1981.
7. B. I. Spinrad. "Unconventional Liquid Metal Cooled Fast Power Reactor Concepts". Progress Report to U.S. Department of Energy, 1986.
8. D. Broadley and R. N. McSweeney. "Sizing of Decay Heat Rejection Loops for LMFBRs". In Proceedings of International Conference, pp. 117-124. The British Energy Society, London, 1978.
9. F. P. Incropera and D. P. DeWitt. Fundamentals of Heat and Mass Transfer. 2nd edition. John Wiley & Sons, New York, 1985.
10. E. M. Sparrow and R. D. Cess. Radiation Heat Transfer. Augmented edition. Hemisphere Publishing Co., Washington, 1981.

11. S. Glasstone and A. Sesonske. Nuclear Reactor Engineering. 3rd edition. Van Nostrand Reinhold Co., New York, 1981.
12. S.K. Chung. "Fission product after-heat in Fast Breeder Reactors". M.S. Thesis, Iowa State University, 1985.
13. American Nuclear Society. "Decay Heat Power in Light Water Reactors". Proposed ANS Standard 5.1, 1978.

8. ACKNOWLEDGEMENT

I want to express my gratitude and appreciation to all who have helped me in completing the work and in preparing this thesis.

First, I want to thank Prof. M. M. Razzaque who has constantly advised, encouraged and helped me.

I also want to thank Prof. B. I. Spinrad, Head of the Nuclear Engineering Department, Prof. A. F. Rohach and Prof. M. B. Pate who provided useful comments and suggestions throughout the duration of the present work. I also want to acknowledge Dr. John Sankoorikal, Mr. Randy Schmidt, Mr. Joe Lofshult and Mr. Rajendra Patil for giving useful information and hints.

Besides, all those who have contributed in one way or another to the present work and are not mentioned above, are also acknowledged and thanked.

I want to take this opportunity to gratefully acknowledge the U. S. Department of Energy for sponsoring this project.

(Anil P. Macwan)

9. APPENDIX A. CALCULATION OF RALEIGH NUMBER FOR THE INNER CHANNEL

The Raleigh number is defined as shown in equation (9.1). It is a product of Grashof number and Prandtl number.

$$Ra = GrPr \quad (9.1)$$

$$Gr_x = \frac{g\beta x^3 (T_w - T_g)}{\nu} \quad (9.2)$$

where x is the height, g is the acceleration due to gravity, β is the volumetric thermal expansion coefficient, ν is the kinematic viscosity of the gas given as the ratio of the viscosity μ and density ρ , and T_w and T_g are the temperatures of the reactor walls and the gas in the inner channel, respectively.

Using the properties for Nitrogen, the Grashof number (Gr) was calculated for various heights in the inner channel. The results of these calculations are shown in Table 1. Values of Raleigh number (Ra) are also given in the table.

The critical value of Ra when the flow becomes turbulent is approximately 10^9 . Thus, it can be seen from the Table 1 that the flow in the inner channel might become turbulent before it reaches the height of 2.0 m.

TABLE 1. Values of Gr and Ra for the Inner Channel

Height in Inner Channel	Grashof Number	Raleigh Number
1.0 m	2.4×10^8	1.7×10^8
2.0 m	1.9×10^9	1.4×10^9
3.0 m	6.5×10^9	4.6×10^9
9.0 m	1.8×10^{11}	1.3×10^{11}
18.0 m	1.4×10^{12}	1.0×10^{12}

10. APPENDIX B. COMPARISON OF HEAT GENERATION TERM USED IN
PRESENT ANALYSIS WITH TABULATED RESULTS

The semi-empirical relation for the decay heat generation as a function of time after shutdown that has been used in the analysis is given by [6]

$$P(\theta) = 0.134P_0\theta^{-0.285} \quad (10.1)$$

where $P(\theta)$ is the decay heat generation rate at time θ seconds after shutdown, while P_0 is the reactor operating power assuming that the reactor has been operating for very long time before shutdown.

The tabulated values of the fraction of the decay heat at time θ are obtained from the ref. [5]. The Table 2 shows a comparison of the two values.

TABLE 2. Comparison of Decay Heat Calculated from semi-empirical correlation and Obtained from Table in ref. [5]

$P(\theta)/P_0$		
Time After Shutdown	Calculated using equation (10.1)	Obtained from ref [5]
1 sec	0.134	0.062
10 sec	0.0695	0.050
100 s	0.036	0.035
1 hr	0.013	0.015
1 day	0.0052	0.0045

11. APPENDIX C. FORMULA FOR VIEW FACTOR BETWEEN REACTOR
WALLS AND BAFFLE

The view factor between the reactor walls and the baffle is taken from the formula for view factor F_{1-2} between two finite thin parallel plates 1 and 2 both having the same dimensions of length l and width w , c being the distance separating the two plates [10].

$$\begin{aligned}
 F_{1-2} \left(\frac{\pi XY}{2} \right) &= \ln \left(\frac{(1 + X^2)(1 + Y^2)}{1 + X^2 + Y^2} \right) \\
 &+ Y\sqrt{1 + X^2} \tan^{-1} \left(\frac{Y}{\sqrt{1 + X^2}} \right) \\
 &+ X\sqrt{1 + Y^2} \tan^{-1} \left(\frac{X}{\sqrt{1 + Y^2}} \right) \\
 &- X \tan^{-1}(X) - Y \tan^{-1}(Y)
 \end{aligned}$$

where $X = l/c$, and $Y = w/c$.

12. APPENDIX D. PROGRAM TO PERFORM ITERATIVE PROCEDURE

```

C PROGRAM TO CALCULATE THE AMOUNT OF HEAT TAKEN UP BY AIR
C BY NATURAL CONVECTION, USING DITTUS-BOELTER CORRELATION
REAL TOTHT, TOTLT, TOTW, D, DE, HTNODE, ANODE, AF, G, K, CP, MU1
REAL TIN, TOUT, T1, T2, RHO1, RHO2, RHOAV, RHOIN, RHOOUT, MUW, MUAV
REAL TGUSS, NUM, DEN, VAV, M, V1, RE, H, QNODE, QTOT, HTT
REAL EPSILON, OMEGA, MUIN, MUOUT, MU, BAFGAP
OPEN(1, FILE='OUT.DAT', STATUS='NEW')
C DIMENSIONS OF THE REACTOR VESSEL.
C THE USER IS PROMPTED FOR THE DIMENSIONS OF THE TANK.
PRINT*, ' INPUT THE DIMENSIONS OF THE REACTOR VESSEL'
PRINT*, ' LENGTH WIDTH HEIGHT, all in Meters'
READ*, TOTLT, TOTW, TOTHT
C THE USER IS PROMPTED FOR THE GAP BETWEEN WALLS AND BAFFLE.
PRINT*, ' INPUT THE GAP BETWEEN REACTOR WALLS & BAFFLE in ft'
READ*, BAFGAP
D = 0.3048*BAFGAP
DE = 2.*D
HTNODE = 1.0
ANODEW = 2.*HTNODE*TOTLT + 2.*HTNODE*TOTW
ANODEB = 2.*HTNODE*(TOTLT+DE) + 2.*HTNODE*(TOTW+DE)
AF = (TOTLT + TOTW + DE)*DE
C PROPERTIES OF THE FLUID (NITROGEN)
G = 9.81
K = 0.0259
CP = 2069.01
MU = 1.787E-05
C RADIATIVE PROPERTIES AND CONSTANTS
SIGMA = 5.68E-08
C THE USER IS PROMPTED FOR THE WALL EMISSIVITY
PRINT*, ' PLEASE INPUT THE WALL EMISSIVITY'
PRINT*, ' A NUMBER > 0.0 AND < OR = 1.0'
READ*, EM
C THE USER IS PROMPTED TO INPUT THE VALUE OF OMEGA, i.e. RATIO
C OF ENTRANCE-EXIT PRESSURE DROP TO TOTAL PRESSURE DROP.
PRINT*, ' INPUT OMEGA, i.e. RATIO OF ENTRANCE-EXIT PRESSURE DROP'
PRINT*, ' TO THE TOTAL PRESSURE DROP'
PRINT*, ' A NUMBER BETWEEN 0.4 and 0.8'
READ*, OMEGA
C THE USER IS PROMPTED FOR THE WALL TEMPERATURE.
PRINT*, ' INPUT THE REACTOR WALL TEMPERATURE in deg F'
READ*, TW
TW = (TW - 32.0)/1.8
CALL VISCOSITY(TW, MUW)
C THE USER IS PROMPTED FOR CHANNEL INLET GAS TEMPERATURE
PRINT*, ' ENTER THE INLET TEMPERATURE FOR THE INNER CHANNEL'
PRINT*, ' in deg F'
READ*, TIN
TIN = (TIN - 32.0)/1.8
CALL DENSITY (TIN, RHOIN)
CALL VISCOSITY(TIN, MUIN)

```

```

C   GUESS BAFFLE TEMPERATURE AS 273.0 C
    TBOLD = 273.0
C   CONVERT TBOLD FORM deg C to deg F.
    TBOLDF = TBOLD*1.8 + 32.0
C   Y IS THE RELAXATION PARAMETER FOR THE CONVERGENCE OF TBOLD.
C   ASSUME Y = 0.1 (i.e. UNDERRELAXATION)
    Y = 0.1
C   GUESS OUTLET TEMPERATURE = 170.0 F
550   TGUSS = 170.0
    TGUSS = (TGUSS - 32.0)/1.8
450   CALL DENSITY(TGUSS,RHOOUT)
    CALL VISCOSITY(TGUSS,MUOUT)
    RHOAV = (RHOIN + RHOOUT)/2.0
    MUAV = (MUIN + MUOUT)/2.0
    NUM = 0.5 *(RHOIN - RHOOUT)*G*DE*(1.0 - OMEGA)
    DEN = 0.158*((DE*RHOAV)/MUAV)**(-0.25)*RHOAV
    VAV = (NUM/DEN)**0.5714
    M = VAV*RHOAV*AF
    T1 = TIN
    HTT = 0.0
    QTOT = 0.0
    T2SUM = 0.0
    I = 1
150  CALL DENSITY(T1,RHO1)
    V1 = M/(RHO1*AF)
    CALL VISCOSITY(T1,MU1)
    RE = (DE*V1*RHO1)/MU1
    H = 0.02*(K/HTNODE)*RE**(0.8)*(MU1/MUW)**0.14
    QCONVW = H*ANODEW*(TW - T1)
    QCONVB = H*ANODEB*(TBOLD - T1)
    QNODTOT = QCONVW + QCONVB
    FRACBAF = QCONVB/QNODTOT
    QTOT = QTOT + QNODTOT
    T2 = QNODTOT/(M*CP) + T1
    T2SUM = T2SUM + T2
    T1 = T2
    I = I + 1
    HTT = HTT + HTNODE
    IF(HTT.GE.TOTHT) THEN
        GO TO 250
    ELSE
        GO TO 150
    ENDIF
250  EPSILON = (TGUSS - T2)/TGUSS
    EPSILON = ABS(EPSILON)
    IF (EPSILON.LE.1.0E-03) THEN
        GO TO 350
    ELSE
        TGUSS = T2
        GO TO 450

```

```

PRINT*, 'OUTLET TEMPERATURE = ', T2, ' C'
PRINT*, 'BAFFLE GAP = ', D/0.3048
PRINT*, 'BAFFLE TEMPERATURE = ', TBNEW
PRINT*, 'TOTAL HEAT REMOVAL = ', QTOTMW, 'MW'
PRINT*, ' CALCULATIONS OVER'
CLOSE(1)
STOP
END

```

C
C

```

SUBROUTINE DENSITY(T, RHO)
REAL T, TK, RHO, C0, C1, C2, C3, C4, C5
C0 = 4.6942
C1 = -2.6089E-02
C2 = 7.4358E-05
C3 = -1.1321E-07
C4 = 8.5135E-11
C5 = -2.3316E-14
TK = T + 273.0
RHO = C0 + C1*TK + C2*TK**2 + C3*TK**3 + C4*TK**4 + C5*TK**5
RETURN
END

```

C
C

```

SUBROUTINE TBAFL(HT, LT, W, DE, K, MU, EM, M, TA, TW, TB1, TB2, QRAD)
C THIS SUBROUTINE CALCULATES NEW BAFFLE TEMPERATURE
C BY INPUTTING THE OLD VALUE AND EQUATING THE RADIATION FROM
C OUTER WALLS OF THE REACTOR TO THE BAFFLE TO THE HEAT CONVECTED
C FROM THE BAFFLE TO THE GAS
REAL HT, LT, W, DE, ABAFW, ABAFLT, ABAFTOT
REAL MU, K, M, SIG, EMIS, NUM, TERM, RE, H, FBAFW, FBAFLT
REAL TA, TW, TWK, TB1, TB1K, TB2, QRAD, EPSILON
X = 0.1
AF = (LT + W + DE)*DE
ABAFW = (W + DE)*HT
ABAFLT = (LT + DE)*HT
ABAFTOT = 2.0*(ABAFW + ABAFLT)
TERM = M/AF
RE = (DE*TERM)/MU
H = (K/HT)*(RE**0.8)
CALL VIEWFCTR(HT, LT+DE, DE/2, FBAFLT)
CALL VIEWFCTR(HT, W+DE, DE/2, FBAFW)
SIGMA = 5.68E-08
NUM = (FBAFW*ABAFW + FBAFLT*ABAFLT)*2.0*SIGMA
TWK = TW + 273.0
C TO RETAIN THE VALUE OF TB1, REDEFINE TB1 AS TBO
TBO = TB1
150 TBOK = TBO + 273.0
QRAD = (NUM/((2.0/EM)-1.0))*(TWK**4-TBOK**4)
TB2 = QRAD/(H*ABAFTOT) + TA

```

```

ERRTB = (TBO - TB2)/TBO
ERRTB = ABS(ERRTB)
IF (ERRTB.LT.1.0E-02) THEN
GO TO 250
ELSE
TBO = TBO + X*(TB2-TBO)
GO TO 150
ENDIF
250 RETURN
END
C
C
SUBROUTINE VIEWFCTR(A,B,C,F)
REAL A,B,C,F,PI,TERM1,TERM2,TERM3,TERM4,TERM5
PI = 3.141592654
X = A/C
Y = B/C
TERM1=ALOG(SQRT((1+X**2)*(1+Y**2)/(1+X**2+Y**2)))
TERM2=X*(SQRT(1+Y**2))*ATAN(X/(SQRT(1+Y**2)))
TERM3=Y*(SQRT(1+X**2))*ATAN(Y/(SQRT(1+X**2)))
TERM4 = X*ATAN(X)
TERM5 = Y*ATAN(Y)
F = (2./(PI*X*Y))*(TERM1+TERM2+TERM3-TERM4-TERM5)
RETURN
END
C
C
SUBROUTINE VISCOSITY(T,MU)
C THIS SUBROUTINE CALCULATES VISCOSITY FOR A GIVEN TEMPERATURE
REAL T, MU, X0, X1, X2, X3, X4, X5
X0 = 16.60471
X1 = 0.04372
X2 = -7.3190E-06
X3 = -8.3291E-08
X4 = 1.8109E-10
X5 = -1.1223E-13
MU = X0 + X1*T + X2*T**2 + X3*T**3 + X4*T**4 + X5*T**5
C THIS MU IS IN MICRPOISES
MU = MU*1.0E-06
C THIS MU IS IN POISES
RETURN
END

```


13. APPENDIX E. PROGRAM USING ODEPACK TO SOLVE DIFFERENTIAL
EQUATION 3.38

```

C      THIS IS A PROGRAM TO SOLVE AN INITIAL VALUE PROBLEM
C      THE PROGRAM CALLS ODEPACK FROM LIBRARY PORT3.
C      THE PROGRAM SOLVES THE FOLLOWING EQUATION:
C       $DY/DT = K1*T^{(-0.285)} - K2*Y - K3.$ 
C      ON THE INTERVAL FROM T = 1 TO T = 18000 sec, WITH INITIAL
C      CONDITION Y = 900.0 deg F, at T = 1 sec.
      EXTERNAL FEX
      DOUBLE PRECISION ATOL, RWORK, RTOL, T, TOUT, Y
      DIMENSION RWORK(70), IWORK(23)
      NEQ=1
      Y = 755.22
      T = 1.00
      TOUT = 101.0
      ITOL = 1
      RTOL = 1.0D-6
      ATOL = 1.0D-10
      ITASK = 1
      ISTATE = 1
      IOPT = 0
      LRW = 70
      LIW = 23
      JT = 2
      DO 40 IOUT = 1,180
          CALL LSODA(FEX,NEQ,Y,T,TOUT,ITOL,RTOL,ATOL,ITASK,ISTATE,
1          IOPT,RWORK,LRW,IWORK,LIW,JDUM,JT)
          Y1 = Y
          WRITE(10,20)T,Y1 - 273.0
20          FORMAT(E12.4,E14.6)
          IF (ISTATE .LT. 0) GO TO 80
40          TOUT = TOUT + 1.0D2
          WRITE(6,60)IWORK(11), IWORK(12), IWORK(13),IWORK(19),RWORK(15)
60          FORMAT(/2X,'NO. STEPS =',I4,2X,'NO. F-S =',I4,2X,'NO. J-S =',I4/
1 2X,'METHOD LAST USED =',I2,2X,'LAST SWITCH WAS AT T =',E12.4)
          STOP
80          WRITE(6,90)ISTATE
90          FORMAT(///2X,'ERROR HALT.. ISTATE =',I3)
          STOP
      END
C
      SUBROUTINE FEX (NEQ, T, Y, YDOT)
      DOUBLE PRECISION T, Y, YDOT
      REAL K,L,M,NU,NUS,K1,K2,K3
      SLOPE = 0.0225
      INTRCP = -11.2380
      L = 21.0
      HT = 18.0
      W = 4.0
      V = L*HT*W
      V = V*35.31
      RHO = 52.35

```

```
M = RHO*V
PO = 800.0
CP = 0.3022
TERM = M*CP*(1.8991E-03)
K1 = 0.137*PO/(TERM)
K2 = SLOPE/(TERM)
K3 = INTRCP/(TERM)
YDOT = K1*T**(-0.285) - K2*Y - K3
RETURN
END
```

14. APPENDIX F. RESULTS OF COMPUTATIONS USING ITERATIVE
PROCEDURE

TABLE 3. Effect of D and T_w on Heat Removal Rate

Heat Removal Rate, MW			
T_w , ° F	900.00	950.00	1000.00
° C	482.22	510.00	537.78
$D = 1.0$ ft	3.9270	4.3357	4.7488
1.5 ft	5.7259	6.3411	6.9739
2.0 ft	7.3139	8.1340	9.0009
3.0 ft	10.2966	11.4427	12.6485
$\epsilon = 0.7$, $\Omega = 0.5$ and $T_{g,i} = 37.78^\circ$ C			

TABLE 4. Effect of ϵ and T_w on Heat Removal Rate

Heat Removal Rate, MW			
T_w , ° F	900.00	950.00	1000.00
° C	482.22	510.00	537.78
$\epsilon = 0.6$	5.3169	5.9095	6.5298
0.7	5.7259	6.3411	6.9739
0.8	6.0789	6.7360	7.4177
0.9	6.4396	7.1194	7.8197
1.0	6.7761	7.4696	8.1799
$D = 1.5$ ft, $\Omega = 0.5$ and $T_{g,i} = 37.78^\circ$ C			

TABLE 5. Effect of Ω and T_w on Heat Removal Rate

Heat Removal Rate, MW			
T_w , ° F	900.00	950.00	1000.00
° C	482.22	510.00	537.78
$\Omega = 0.4$	6.0353	6.7030	7.3569
0.5	5.7259	6.3411	6.9739
0.6	5.3652	5.9185	6.5249
0.7	4.8994	5.4282	5.9770
0.8	4.3315	4.7906	5.2653

$D = 1.5$ ft, $\epsilon = 0.7$, and $T_{g,i} = 37.78^\circ$ C

TABLE 6. Effect of $T_{g,i}$ and T_w on Heat Removal Rate

Heat Removal Rate, MW			
T_w , ° F	900.00	950.00	1000.00
° C	482.22	510.00	537.78
$T_{g,i} = 37.78^\circ$ C	6.0353	6.7030	7.3569
48.89° C	5.2483	5.8092	6.4239
60.00° C	4.8055	5.3385	5.9194
71.11° C	4.3868	4.9124	5.4576

$D = 1.5$ ft, $\epsilon = 0.7$, and $\Omega = 0.5$.

TABLE 7. Effect of D and T_w on Baffle Temperature

Baffle Temperature, ° C			
T_w , ° F	900.00	950.00	1000.00
° C	482.22	510.00	537.78
D = 1.0 ft	322.08	352.04	382.15
1.5 ft	245.38	272.55	301.54
2.0 ft	191.85	213.99	237.48
3.0 ft	126.61	102.47	114.78
$\epsilon = 0.7, \Omega = 0.5$ and $T_{g,i} = 37.78^\circ \text{C}$			

TABLE 8. Effect of ϵ and T_w on Baffle Temperature

Baffle Temperature, ° C			
T_w , ° F	900.00	950.00	1000.00
° C	482.22	510.00	537.78
$\epsilon = 0.6$	212.53	236.42	261.74
0.7	245.38	272.55	301.54
0.8	278.66	306.69	336.09
0.9	307.43	336.64	366.52
1.0	333.44	363.29	393.70
D = 1.5 ft, $\Omega = 0.5$ and $T_{g,i} = 37.78^\circ \text{C}$			

TABLE 9. Effect of Ω and T_w on Baffle Temperature

Baffle Temperature, ° C			
T_w , ° F	900.00	950.00	1000.00
° C	482.22	510.00	537.78
$\Omega = 0.4$	234.39	259.83	288.87
0.5	245.38	272.55	301.53
0.6	258.96	288.45	316.76
0.7	278.78	306.85	336.27
0.8	302.72	332.08	361.98

$D = 1.5 \text{ ft}$, $\epsilon = 0.7$, and $T_{g,i} = 37.78^\circ \text{ C}$

TABLE 10. Effect of $T_{g,i}$ and T_w on Baffle Temperature

Baffle Temperature, ° C			
T_w , ° F	900.00	950.00	1000.00
° C	482.22	510.00	537.78
$T_{g,i} = 37.78^\circ \text{ C}$	245.38	259.83	288.87
48.89° C	257.23	286.39	314.62
60.00° C	268.99	298.75	327.22
71.11° C	282.50	310.40	338.99

$D = 1.5 \text{ ft}$, $\epsilon = 0.7$, and $\Omega = 0.5$

TABLE 11. Effect of D and T_w on Outlet Gas Temperature

Outlet Gas Temperature, ° C			
T_w , ° F	900.00	950.00	1000.00
° C	482.22	510.00	537.78
D = 1.0 ft	66.58	68.53	70.47
1.5 ft	60.90	62.62	64.14
2.0 ft	57.25	58.67	60.11
3.0 ft	52.99	54.08	55.19
$\epsilon = 0.7, \Omega = 0.5$ and $T_{g,i} = 37.78^\circ \text{C}$			

TABLE 12. Effect of ϵ and T_w on Outlet Gas Temperature

Outlet Gas Temperature, ° C			
T_w , ° F	900.00	950.00	1000.00
° C	482.22	510.00	537.78
$\epsilon = 0.6$	59.79	61.39	63.01
0.7	60.90	62.52	64.14
0.8	61.84	63.53	65.24
0.9	62.78	64.50	66.23
1.0	63.64	65.37	67.09
D = 1.5 ft, $\Omega = 0.5$ and $T_{g,i} = 37.78^\circ \text{C}$			

TABLE 13. Effect of Ω and T_w on Outlet Gas Temperature

Outlet Gas Temperature, ° C			
T_w , ° F	900.00	950.00	1000.00
° C	482.22	510.00	537.78
$\Omega = 0.4$	60.13	61.73	63.26
0.5	60.90	62.52	64.14
0.6	61.88	63.50	65.23
0.7	63.09	64.87	66.67
0.8	64.98	66.87	68.75

$D = 1.5$ ft, $\epsilon = 0.7$, and $T_{g,i} = 37.78^\circ$ C

TABLE 14. Effect of $T_{g,i}$ and T_w on Outlet Gas Temperature

Outlet Gas Temperature, ° C			
T_w , ° F	900.00	950.00	1000.00
° C	482.22	510.00	537.78
$T_{g,i} = 37.78^\circ$ C	60.90	62.52	64.14
48.89° C	71.61	73.19	74.88
60.00° C	82.34	83.92	85.62
71.11° C	92.94	94.63	96.33

$D = 1.5$ ft, $\epsilon = 0.7$, and $T_{g,i} = 37.78^\circ$ C

15. APPENDIX G. RESULTS OF COMPUTATIONS USING ODEPACK

TABLE 15. T_w as a function of θ with no cooling

Wall Temperature, ° C	
$\theta = 101$ sec	484.72
1 hr	515.48
2 hr	536.87
3 hr	555.27
4 hr	571.98
5 hr	587.52

TABLE 16. T_w as a function of θ and D

Wall Temperature, ° C				
D	1.0 ft	1.5 ft	2.0 ft	3.0 ft
$\theta = 101$ sec	484.45	484.34	484.22	484.03
1 hr	505.62	501.40	496.12	490.26
2 hr	516.66	508.18	499.34	486.47
3 hr	524.41	511.73	498.73	480.20
4 hr	530.24	513.45	496.51	472.87
5 hr	534.73	513.95	493.32	465.10

$\epsilon = 0.7, \Omega = 0.5$ and $T_{g_i} = 37.78^\circ \text{C}$

TABLE 17. T_w as a function of θ and ϵ

Wall Temperature, ° C			
ϵ	0.6	0.7	0.8
$\theta = 101$ sec	484.37	484.34	484.33
1 hr	502.58	501.40	500.90
2 hr	510.50	508.18	507.17
3 hr	515.14	511.73	510.22
4 hr	517.89	513.45	511.46
5 hr	519.39	513.95	511.50
ϵ	0.9	1.0	
$\theta = 101$ sec	484.29	484.27	
1 hr	499.73	498.89	
2 hr	504.88	503.29	
3 hr	506.86	504.46	
4 hr	507.07	503.29	
5 hr	506.15	502.26	
D = 1.5 ft, $\Omega = 0.5$ and $T_{g,i} = 37.78^\circ$ C			

TABLE 18. T_w as a function of θ and Ω

Wall Temperature, ° C			
Ω	0.4	0.5	0.6
$\theta = 101$ sec	484.28	484.34	484.36
1 hr	499.22	501.40	502.07
2 hr	503.90	508.18	509.53
3 hr	505.45	511.73	513.74
4 hr	505.26	513.45	516.10
5 hr	503.95	513.95	517.22

Ω	0.7	0.8
$\theta = 101$ sec	484.36	484.42
1 hr	502.24	501.43
2 hr	509.89	514.26
3 hr	514.30	520.81
4 hr	516.87	525.45
5 hr	518.18	528.77

$D = 1.5$ ft, $\epsilon = 0.7$ and $T_{g,i} = 37.78^\circ$ C

TABLE 19. T_b as a function of θ and D

Baffle Temperature, ° C				
D	1.0 ft	1.5 ft	2.0 ft	3.0 ft
$\theta = 101$ sec	324.51	247.54	193.49	127.68
1 hr	347.40	264.78	203.92	131.29
2 hr	359.34	271.63	205.91	129.10
3 hr	367.72	275.22	205.41	125.46
4 hr	374.02	276.95	203.59	121.21
5 hr	378.88	277.46	200.97	116.71

$\epsilon = 0.7$, $\Omega = 0.5$ and $T_{g,i} = 37.78^\circ$ C

TABLE 20. T_b as a function of θ and ϵ

Baffle Temperature, ° C			
ϵ	0.6	0.7	0.8
$\theta = 101$ sec	214.45	247.54	280.85
1 hr	230.58	264.78	297.99
2 hr	237.59	271.63	304.47
3 hr	241.70	275.22	307.62
4 hr	244.14	276.95	308.90
5 hr	245.46	277.46	308.94
ϵ	0.9	1.0	
$\theta = 101$ sec	309.62	335.65	
1 hr	326.04	351.51	
2 hr	331.51	356.23	
3 hr	333.62	357.55	
4 hr	333.85	357.00	
5 hr	332.87	355.27	

$D = 1.5$ ft, $\Omega = 0.5$ and $T_{g,i} = 37.78^\circ$ C

TABLE 21. T_b as a function of θ and Ω

Baffle Temperature, ° C			
Ω	0.4	0.5	0.6
$\theta = 101$ sec	236.40	247.54	261.19
1 hr	251.05	264.78	279.62
2 hr	255.71	271.63	287.38
3 hr	257.16	275.22	291.76
4 hr	256.97	276.95	294.22
5 hr	255.68	277.46	295.38

Ω	0.7	0.8
$\theta = 101$ sec	280.99	305.09
1 hr	299.49	326.43
2 hr	307.40	336.92
3 hr	311.97	343.90
4 hr	314.63	348.85
5 hr	315.99	352.39

$D = 1.5$ ft, $\epsilon = 0.7$ and $T_{g,i} = 37.78^\circ$ C

TABLE 22. $T_{g,o}$ as a function of θ and D

Outlet Gas Temperature, ° C				
D	1.0 ft	1.5 ft	2.0 ft	3.0 ft
$\theta = 101$ sec	66.73	61.09	57.38	53.07
1 hr	68.21	62.09	58.03	53.32
2 hr	68.98	62.48	58.16	53.17
3 hr	69.53	62.69	58.13	52.92
4 hr	69.93	62.79	58.01	52.63
5 hr	70.25	62.82	57.85	52.32

$\epsilon = 0.7$, $\Omega = 0.5$ and $T_{g,i} = 37.78^\circ$ C

TABLE 23. $T_{g,o}$ as a function of θ and ϵ

Outlet Gas Temperature, ° C			
ϵ	0.6	0.7	0.8
$\theta = 101$ sec	59.90	61.09	61.96
1 hr	60.96	62.09	62.98
2 hr	61.41	62.48	63.36
3 hr	61.68	62.69	63.55
4 hr	61.84	62.79	63.62
5 hr	61.93	62.82	63.63
ϵ	0.9	1.0	
$\theta = 101$ sec	62.88	63.76	
1 hr	63.84	64.67	
2 hr	64.16	64.95	
3 hr	64.28	65.02	
4 hr	64.30	64.99	
5 hr	64.24	64.89	
D = 1.5 ft, $\Omega = 0.5$ and $T_{g,i} = 37.78^\circ$ C			

TABLE 24. T_{g_o} as a function of θ and Ω

Outlet Gas Temperature, ° C			
Ω	0.4	0.5	0.6
$\theta = 101$ sec	60.22	61.09	61.99
1 hr	61.06	62.09	63.05
2 hr	61.33	62.48	63.50
3 hr	61.41	62.69	63.76
4 hr	61.40	62.79	63.90
5 hr	61.33	62.82	63.97
Ω	0.7	0.8	
$\theta = 101$ sec	63.24	65.14	
1 hr	64.40	66.50	
2 hr	64.89	67.16	
3 hr	65.18	67.61	
4 hr	65.34	67.92	
5 hr	65.43	68.15	
D = 1.5 ft, $\epsilon = 0.7$ and $T_{g_i} = 37.78^\circ$ C			